Analysis of a shark reveals ancient habenular asymmetries in gnathostomes and points to Wnt regulation as a driving force in their diversification

Maxence Lanoizelet[1*], Léo Michel[1*], Ronan Lagadec[1*], Hélène Mayeur[1*], Lucile Guichard[1*], Dany Séverac[2], Kyle Martin[3], Christophe Klopp[4], Sylvain Marcellini[5], Hector Castillo[5], Nicolas Pollet[6], Eva Candal[7], Mélanie Debiais-Thibaud[8], Catherine Boisvert[9], Bernard Billoud[10], Michael Schubert[11], Patrick Blader[12], Sylvie Mazan[1]

[1]CNRS, Sorbonne Université, UMR7232-Biologie Intégrative des organismes marins (BIOM), Observatoire Océanologique, Banyuls sur Mer, France
[2]MGX, Université Montpellier, CNRS, INSERM, 34094 Montpellier, France
[3]UK Research and Innovation, Biotechnology and Biological Sciences Research Council Affiliations, UK
[4]Plateforme Bioinformatique, Genotoul, BioinfoMics, UR875 Biométrie et Intelligence Artificielle, INRAE, Castanet-Tolosan, France
[5]Department of Cell Biology, School of Biological Sciences, University of Concepcion, Chile
[6]Université Paris-Saclay, CNRS, IRD, Évolution, Génomes, Comportement et Écologie, Université Paris-Saclay, Gif-sur-Yvette, France.
[7]Departament of Functional Biology, CIBUS, Faculty of Biology, Universidade de Santiago de Compostela, 15782, Santiago de Compostela, Spain
[8]ISEM, Université de Montpellier, CNRS, IRD, EPHE, Montpellier, France
[9]School of Molecular and Life Sciences, Curtin University, Perth, WA, Australia.
[10]UMR8227, CNRS-Sorbonne Université, Station Biologique, Place Georges Teissier, 29680 Roscoff, France
[11]Laboratoire de Biologie du Développement de Villefranche-sur-Mer (LBDV), Institut de la Mer de Villefranche, Sorbonne Université, CNRS, 06230 Villefranche-sur-Mer, France
[12]Centre de Biologie Intégrative (CBI, FR 3743), Université de Toulouse, CNRS, UPS, France

[*] Authors contributed equally to this work

Corresponding author: Sylvie Mazan, mazan@obs-banyuls.fr

ABSTRACT

In order to gain insight into the origin and mode of evolution of asymmetries in the vertebrate habenula, we have used combinations of transcriptomic and functional approaches in a cartilaginous fish, the catshark *Scyliorhinus canicula*. We find that catshark habenulae harbor marked asymmetries not only in the medial habenulae as in the zebrafish, but also in the lateral habenulae, which differ extensively by their neuronal identities. Comparisons across a broad sampling of gnathostomes suggest that the latter reflect an ancestral gnathostome trait, independently lost in tetrapods and neopterygians. Analysis of underlying mechanisms in the catshark highlight an asymmetric temporal control of neurogenesis in the medial habenulae and a central role of Wnt signaling in the elaboration of asymmetries in the lateral ones. The pathway is submitted to a highly dynamic, asymmetric regulation during habenula development, with a Nodal dependent left repression at a stage when precursors for lateral habenulae have exited cell cycles. Using a pharmacological approach during this time window, we show that Wnt activity promotes lateral right neuronal identities in the lateral right habenula, while its repression by Nodal in the lateral left habenula promotes lateral left neuronal identities. Based on comparisons of these data with those reported in the zebrafish and in the mouse, we propose that habenular asymmetry formation and diversification in gnathostomes rely on a same developmental logic, involving a conserved temporal regulation of neurogenesis, which shapes neuronal identities on both sides and is asymmetrically modified by a dynamic Wnt activity, right restricted in the ancestral state and prone to variations in time and space during evolution.

INTRODUCTION

Habenulae are bilateral epithalamic structures, present in all vertebrates. They appear as a key node in conserved circuits connecting various forebrain areas to midbrain nuclei, and integrate information from multiple sources, including sensory organs and corticolimbic areas, to regulate complex behavioural, cognitive and emotional responses[1–4]. A basic architecture of this structure into two domains (medial and lateral in mammals, dorsal and ventral in teleosts), exhibiting distinct molecular properties and connectivity patterns, is known to be conserved across gnathostomes[5,6] but more precise comparisons of neuronal populations across vertebrates remain difficult, despite the availability of detailed single cell RNA-seq maps in the mouse and the zebrafish[7,8]. A unique feature of this structure in the vertebrate brain is that in many species including human, it displays asymmetries between the left and the right sides[9,10]. Their biological significance has started to emerge in the zebrafish, the reference model for analyses of both their roles and mechanisms of formation[11]. In this species, sensory cues are differentially processed between the right and left habenulae, and asymmetries have been shown to impact important adaptive responses such as exploratory and food-seeking behaviours, light preference or responses to fear[12–15.]. Despite the evolutionary relevance of these functions depending on ecological context, the origin and mode of diversification of habenular asymmetries across vertebrates remains unclear. Morphological characterizations suggest that they considerably vary in nature -size, cellular or nuclei organisation, connectivity pattern- and degree across vertebrates[10]. In line with this notion, more detailed molecular characterizations, essentially focused on teleosts thus far, highlight complex presence/absence patterns of asymmetric traits, suggestive of a rapid drift in this taxon[16,17]. However, whether habenular asymmetries in teleosts reflect the vertebrate or gnathostome ancestral state is unclear since they may employ highly divergent mechanisms for their formation[18]. In the zebrafish, habenular asymmetries are restricted to the dorsal habenula (dHb), consisting in different relative proportions between lateral and medial subdomains (dHbl and dHbm respectively), respectively prevailing on the left and on the right[19–21]. Analyses of the mechanisms controlling their formation have highlighted a pivotal role of Wnt signaling. The pathway activity is submitted to a finely tuned temporal control during habenular development and it controls distinct successive processes, including the specification of the ventral habenula, the regulation of the temporal control of neurogenesis and the choices of neuronal identities in the differentiating dorsal habenula[22–25]. Its repression on the left side via an interaction with the adjacent parapineal during a well defined window time results in the elaboration of habenular asymmetries, and the promotion of right-sided neuronal identities in the right dorsal habenula[24]. Analyses of two non-conventional models harbouring marked habenular asymmetries, the lamprey and catshark, suggest that this mechanism

does not reflect the vertebrate ancestral state, likely to be independent of the parapineal but to crucially involve an early left restricted diencephalic Nodal activity, dispensable in the zebrafish[18]. To clarify the mode of evolution of habenular asymmetries across gnathostomes, we have taken as reference the catshark *Scyliorhinus canicula*, which, as a member of chondrichthyans (cartilaginous fishes), the closest outgroup of osteichthyans, provides a relevant reference to explore their origin[26]. We find that habenulae in this species display a highly asymmetric habenular organization, and has retained ancient asymmetries of jawed vertebrates, lost in the mouse and zebrafish. We also suggest a conserved regulatory logic for their formation, involving interactions between a conserved temporal control of neurogenesis and a more flexible temporal and spatial regulation of Wnt signaling, which could account for the evolvability of habenular asymmetries across vertebrates.

MATERIALS AND METHODS

RNA isolation, library construction and sequencing

Left and right habenulae were manually dissected from a total of 45 anaesthetised stage 31 catshark embryos and stored in RNAlater (Ambion) until RNA extraction. Three left pools, each containing 15 left habenulae and three right ones, containing the corresponding 15 right habenulae, were made from these explants. Total RNA was extracted from these pools using the Ribopure Kit (Ambion). RNA quantities and integrity indexes (RINs) were controlled using a Bioanalyzer 2100 (Agilent). RNA quantities ranging between 1.1 and 2.4 µg and RIN values comprised between 7.4 and 9.6 were obtained for each pool analysed.

Library construction and sequencing

We prepared RNA-seq libraries using the Truseq stranded mRNA sample prep kit (Illumina, San Diego, CA, USA) according to the manufacturer’s instructions. Briefly, polyadenylated RNAs were selected using oligo-dT magnetic beads. The polyA+ RNAs were fragmented using divalent cations at elevated temperature and reverse transcribed using random hexamers, Super Script II (Thermo Fisher Scientific, Carlsbad, CA) and actinomycin D. Deoxy-TTP was replaced by dUTP during the second strand synthesis to prevent its amplification by PCR. Double stranded cDNAs were adenylated at their 3' ends and ligated to Illumina's adapters containing unique dual indexes (UDI). Ligated cDNAs were PCR amplified for 15 cycles PCR and the PCR products were purified using AMPure XP Beads (Beckman Coulter Genomics, Brea, CA, USA). The size distribution of the resulting libraries was monitored using a Fragment Analyzer (Agilent Technologies, Santa Clara, CA, USA) and the libraries were quantified using the KAPA Library quantification kit (Roche, Basel, Switzerland). The libraries were denatured with NaOH, neutralized with Tris-HCl, and diluted to 7.5 pM. Clustering was done on a cBot and sequencing was performed on a HiSeq 2500 (Illumina, San Diego, CA, USA) using the paired-end 2x125 nt protocol on two lanes of a flow cell.

Mapping and expression profiling

Reads obtained from each one of the three left and right habenula pools were pseudo-mapped onto an annotated database of reference gene models[27] (described in Mayeur et al, manuscript in revision) and pseudo-counted using a k-mer quantification method, kallisto[28]. Contigs exhibiting statistically significant count differences between the left and right habenulae were identified using the Wald test implemented in sleuth[29] (q-value threshold 5E-02).

Gene ontology (GO) analysis

Left versus right habenulae GO term enrichment gene analysis was conducted using the ConsensusPathDB online tool[30,31] (http://cpdb.molgen.mpg.de/) against the whole list of genes in the catshark gene models reference. It was restricted to levels 2-5 GO terms related to biological processes (p-value cut-off of 5E-02, further curated to a q-value threshold of 5E-02).

Embryo collection

Scyliorhinus canicula eggs were provided by the Aquariology Service of the Banyuls sur Mer Oceanological Observatory. Embryos were dissected, fixed and staged as described previously[32]. Juvenile of *Lepisosteus oculatus* and *Erpetoichthys calabaricus* were provided from commercial sources (https://www.poisson-or.com/). Juveniles of *Callorhincus milii* were provided by C. Boisvert (Curtin University, Australia) and *Xenopus tropicalis* by S. Marcellini (University of Concepcion, Chile) and N. Pollet (Université Paris-Saclay, France).

***In situ* hybridization (ISH), HCR-FISH and IHC.**

Probes were obtained from collections of embryonic *S. caniParis-Saclay, Francecula* cDNA recombinants[33], or obtained from synthetic double-stranded DNA (Supplementary Table 2). Following ISH, nuclei were counterstained using Nuclear Fast Red (Sigma N3020). Chromogenic ISHs of paraffin sections were conducted using digoxigenin-labelled antisense RNAs as previously described using standard protocols. Fluorescent ISHs were conducted using digoxigenin-labelled antisense RNAs and fluorescein-labelled antisense RNAs as described in[34] . HCR-FISH were conducted as described in[35,36] with slight modifications: slides were incubated 20mn in 10µg/mL PK at RT before probes hybridization. For each genes, probes were designed by Molecular Instrument using the following NCBI accession numbers XM_038775015.1 (*ScKctd12b*), XM_038811423.1 (*ScProx1*) and XM_038818902.1 (*ScSox1*). Amplifiers B3-Alexa Fluor594, B2-Alexa Fluor488 and B1-Alexa Fluor647 were respectively used. Fluorescent immunohistochemical detection of β-catenin (Abcam, Ab6302, 1/1000) on sections was conducted as previously described in[37]. For fluorescent ISHs, HCRs and IHCs, sections were imaged with a Leica SP8 confocal laser-scanning microscope.

BrdU pulse chase analysis.

BrdU pulse labelling and BrdU detection were conducted as described in Lagadec et al. 2018 with the following modifications. Catshark embryos were removed from the egg case, incubated in oxygenated filtrated sea water containing 5 mg/ml BrdU (16.2mM) for 16 hours and for the chase, transferred to filtrated sea water at 16°C until desired stages were reached. Following incubation of sections with the anti-BrdU primary antibody, detection was conducted using m-IgGκ BP-HRP (Santa Cruz; 1/100) and the TSA Plus Cyanine 3 kit (Akoya Bioscience) following suppliers' instructions.

Pharmacological treatments.

For Nodal inhibition, catshark embryos were treated by in ovo injection of 100 µl of a 50µm SB-505124, a selective inhibitor of TGF-β type I receptors Alk4/5/7/18, at stage 16 as previously described[18]. For Wnt inactivation, 100 µl of a DMSO solution containing 1mM IWR-1-endo, a selective inhibitor of tankyrase known to inhibit β-catenin cytoplasmic accumulation through stabilization of the destruction complex member AXIN2, were injected into the egg case at stage 29 and eggs were maintained in oxygenated sea water (16°C) until reaching the desired stage. The same protocol was applied to control embryos, except for the absence of the drug in the injected solution.

RESULTS

Identification of differentially expressed genes between developing left and right catshark habenulae

In order to obtain an unbiased characterization of molecular asymmetries in catshark habenulae, we conducted a transcriptomic comparison between developing left and right habenulae. To this end, we conducted a transcriptomic comparison between these components, focusing on stage 31, when a large fraction of the organ is differentiated but asymmetric pools of neural progenitors persist[37]. Statistical analysis of 362 million read pairs (PE100) obtained from three replicates of left versus right habenulae explants led to the identification of 614 differentially expressed gene models (373 left-enriched and 241 right-enriched), of which 538 can be annotated as protein coding (Fig.1a; Supplementary Table 1). Functional annotation of left- and right-enriched gene lists shows that they share an over-representation of GO (Gene Ontology) terms related to neurogenesis, neuronal differentiation, the formation of neuronal projections and trans-synaptic signalling, as expected for a differentiating brain structure (Supplementary Fig.1a,b; Supplementary Table 1). GO terms selectively over-represented in either one of these two lists are also detected. They include terms related to organismal responses known to be regulated by habenulae, such as the perception of pain, sleep, behavioral fear responses, or to signaling pathways known to be active in habenulae, such as Wnt, opioid receptor, ionotropic glutamate receptor signaling, are also identified (Supplementary

Fig.1c-d). Altogether, these data suggest differential functional specializations of the catshark left and right habenulae.

Catshark habenulae exhibit an asymmetric, lateral to medial subdomain organization

In order to validate asymmetries identified by the transcriptomic analysis and to characterize their spatial organisation, we conducted chromogenic in situ hybridization (ISH) on stage 31 habenulae section for a total of 39 genes selected from the lists of asymmetrically expressed genes (Fig.1a; Supplementary Table 2). Regionalized signals were observed for most of these genes, with three of them showing restricted expressions to neural progenitors, and twenty nine harboring highly specific territories in differentiating habenular subdomains, consistent with expression lateralities predicted by the transcriptomic analysis (Supplementary Fig.2). The latter can be classified into five broad categories, each characterized by largely overlapping expression profiles restricted to (i) the lateral left and (ii) lateral right parts of the habenulae (Supplementary Figure 2b,f), (iii) a broad bilateral medial territory larger on the left than on the right and comprising an anterior dorsal component restricted to the left Supplementary Figure 2d), (iv) left-restricted and (v) right-enriched subdomains located in the external part of the latter (Supplementary Fig.2e,f). More detailed analyses of stage 31 habenulae focusing on five markers of these territories (*ScSox1*, *ScPde1a*, *ScKctd12b*, *ScEnpp2*, *ScProx1*; Fig.1; Supplementary Fig.3 and 4) highlight an organization of the catshark habenulae into three complementary broad subdomains, two lateral ones, respectively referred to as Left- and Right-LHb hereafter and expressing *ScSox1* on the left and *ScProx1* on the right, and a broad bilateral *ScKctd12b* positive medial one, referred to as MHb, also comprising a left restricted anterior component as previously described[18] (Fig.1b2,d,f-k,q,s,u,n,o; Supplementary Fig.3b,d,f; Supplementary Fig.4b,d,f). *ScSox1* and *ScProx1* expressions are almost confined to the left and the right lateral habenulae respectively, except for a small discrete contralateral neuronal population at posterior-most levels of the habenulae. The medial MHb territory is itself partitioned into an internal bilateral component and an external one, adjacent to Left-LHb and Right-LHb (Fig. 1c,e,r,t). The latter is organized into two adjacent territories excluding each other, an anterior, left restricted *ScPde1* territory (Fig.1c,l,r; Supplementary Fig.3c,4c) and a *ScEnpp2* territory, occupying the whole external part of MHb on the right (Fig.1e,m,t; Supplementary Fig.3e,4e). In order to assess whether these asymmetries may reflect transient ones in the differentiating habenulae or definitive neuronal identities of the functional organ, we assessed their maintenance in free feeding juveniles, collected after exhaustion of the yolk reserve (Supplementary Fig.5). The broad expression characteristics and asymmetries of *ScSox1*, *ScPde1a*, *ScKctd12b*, *ScEnpp2* and *ScProx1* were very similar to those observed at stage 31 (Supplementary Fig.5b-j), except for an expansion of *ScEnpp2* signal to the internal component of MHb (Supplementary Fig.5e). Altogether, these

highlight a highly asymmetric organization of the catshark habenulae, both in its lateral and medial subdomains.

Comparisons between the catshark, the mouse and the zebrafish highlight similarities in subdomain signatures, without asymmetry conservations

In order to identify habenular asymmetry or subdomain organization conservations across gnathostomes, we first searched previously reported habenular expression sites for mouse and zebrafish orthologues of markers of the five major territories identified in the catshark. Orthologues of *Kctd8/12a/12b*, which harbor asymmetries in the zebrafish dorsal habenula, were included in this analysis (Supplementary Table 3; Supplementary Figure 6). When documented, most mouse orthologues of catshark MHb markers are expressed in the mouse medial habenula, including *Spon1* and *Trhde*, restricted to the anterior left external component of MHb in the catshark and to a lateral subdomain of the medial habenula in the mouse (Supplementary Fig.6a-c,k). Two out of four gene signatures of Left-LHb in the catshark (*Pcdh17*, *Ntng2*) share a bilateral expression in the mouse lateral habenulae, an expression site also observed for a *Sox1* reporter in *Sox1-LacZ* knock-mice[38]. Mouse orthologues of catshark Right-LHb markers show various profiles spanning the ventral medial habenulae, lateral habenulae and adjacent thalamic nuclei (Supplementary Fig.6f-j), and three of them share a highly specific territory in the paraventricular nucleus of thalamus, ventral to the lateral habenulae (*Rerg*, *Prox1*, *Stxbp6*: Supplementary Fig.6h-j). For comparisons with the zebrafish, we examined the presence of orthologues of catshark territory markers among the gene signatures of scRNA-seq gene clusters mapped to larval or adult habenulae[8]. Orthologues of three catshark asymmetrically expressed MHb markers (*Spon1*, *Kctd8*, *Kctd12a*) also display asymmetric expressions in zebrafish dHb, albeit without consistent laterality conservation. Conversely, with one exception (*prox1a*, part of a dorsal and right enriched cluster), zebrafish orthologues of catshark LHb markers (*Sox1*, *Ak5*, *Kiss1*, *Rerg*, *Prkcq*, *Gng14*) are identified as gene signatures of two bilateral and symmetric, ventral cell clusters of zebrafish larval habenula cell clusters, Hb11 for zebrafish *sox1a/b*, Hb15 (or related adult clusters) for the latter five genes. Taken together, these data support the conservation in the catshark of the subdivision of habenulae in two components (dorsal/medial and ventral/lateral). Intriguingly, they highlight similarities of catshark left-LHB with the mouse lateral habenulae, and of catshark right-LHb with a zebrafish major ventral cell cluster.

Conserved asymmetry patterns can be detected between chondrichthyans, a dipneust and a polypterid in the lateral/ventral habenula

The similarities of catshark left-and right-LHB respectively with the mouse lateral and zebrafish ventral habenulae may reflect taxa specific diversifications of lateral/ventral habenulae, obscuring ancestral traits of habenula organization. In order to test their evolutionary relevance, we used a phylogenetic approach, aimed at reconstructing habenular organization at major gnathostome nodes, taking the catshark as reference. We selected five species for their phylogenetic position in the major gnathostome phyla for this analysis: an holocephalan, the elephant shark *Callorhinchus milii*, two non-teleostean actinopterygians, the reedfish *Erpetoichthys calabaricus* (bichir) and the spotted gar *Lepisosteus oculatus*, and two sarcopterygians, the lungfish *Protopterus annectens* and the frog *Xenopus tropicalis*. In each one of these species, we conducted ISH analysis on transverse sections of habenulae for orthologues of markers of Left-LHb (*Sox1, Ntng2, Pcdh17*), MHb (*Kctd8, Kctd12a, Kctd12b*) and Right-LHb (*Prox1, Kiss1*) in the catshark. Specific habenular expressions were observed in all cases, except for *Kctd12a* in the lungfish, and *Kiss1* in the lungfish and the xenopus, whose expression remained undetectable (Fig.2; Supplementary Fig.7-11). In all species analyzed, profiles of members of the *Kctd8*/*12a*/*12b* family vary among paralogues and across species, but at least one paralogue defines a medial or dorsal habenular territory (Fig.2g-l; Supplementary Fig.7e,g; Supplementary Fig.8f; Supplementary Fig.9f; Supplementary Fig.10e,f; Supplementary Fig.11h,j). Except for a few exceptions (expansion of elephant shark *Kiss1* and *Pcdh17*, reedfish *Prox1*, spotted gar *Ntng2* to various MHb/dHb subterritories), orthologues of catshark Left- and Right-LHb markers are expressed within complementary lateral or ventral territories (Fig.2b-f,n-r; Supplementary Fig.7b-d,h-i; Supplementary Fig.8b-d,g-h; Supplementary Fig.9g-k; Supplementary Fig.10b-d,g; Supplementary Fig.11b-e,g). However, the labeled territories and asymmetry patterns markedly differ between species. As in the catshark, the elephant shark and the reedfish harbor left- and right-restricted lateral/ventral territories, respectively co-expressing *Sox1/Pcdh17/Ntng2* and *Prox1/Kiss1* (Fig.2b,c,n,o; Supplementary Fig.7b-d,h-i; Supplementary Fig.8b-e,g-h). Similarly, in the lungfish, *Sox1*, *Pcdh17* and *Ntng2* share a strong left restricted signal, adjacent to *Kctd8/12b* positive territories with a sharp boundary, while a more discrete lateral *Prox1* positive cell population lining the habenular commissure can be observed on the right side only, in a zone devoid of *PaKctd8/12* expression (Fig.2e,q; Supplementary Fig.10b-d,g). In contrast, expressions of orthologues of both catshark left-and right-LHb markers are bilateral in the spotted gar and the xenopus, albeit with slightly different relative locations between the two species. In the spotted gar, *Pcdh17/Sox1/Ntng2* share an anterior territory, complementary to the *LoProx1/Kiss1* positive one within the left and right ventral habenulae (Fig.2d,p; Supplementary Fig.9b-c,g-k). In the xenopus, their expression is also observed in the left and right habenulae, adjacent and lateral to the *Kctd8/12b* expressing domain (Fig.2f; Supplementary Fig11b-e), while *Prox1* signal is observed in a more ventral and posterior location (Fig.2r; Supplementary Fig.11g).

Wnt signaling activity is dynamic and repressed on the left by Nodal in the catshark developing habenulae

In order to gain insight into the mechanisms controlling the formation of asymmetries shared by chondrichthyans, dipneusts and polypterids in the lateral/ventral habenulae, we focused on the catshark, a model accessible to experimental approaches during development, and on canonical Wnt signaling. *ScLef1* and *ScTcf7l2*, which encode effectors of this pathway, indeed both exhibit statistically significant right enrichments in our transcriptomic analysis (q-value=2.2E-03 and 3.0E-03 respectively). We first characterized the dynamic of Wnt activity during habenula formation, by analyzing the nuclear distribution of β-catenin on histological sections from the first appearance of habenular evaginations (stage 26) to stage 31 (Fig.3; Supplementary Fig.12). At stage 26, β-catenin is broadly distributed in the growing habenular evaginations but a nuclear signal is only observed in some HuC/D positive cells, which form a discrete lateral cell population of differentiating neurons, transiently larger on the left than on the right side at this stage (Fig.3a,b,a1-a4,b1-b4). A broad bilateral cytoplasmic signal is maintained at stage 28, albeit without clear nuclear restriction (Fig.3c,c1-c4). A marked transition is observed at stage 29, with a nuclear accumulation of β-catenin restricted to the lateral right habenula and a withdrawal of the cytoplasmic signal in the lateral left one (Fig.3d,d1-d4). This asymmetry is maintained at stage 31, with a high proportion of positive nuclei in the *Prox1* expressing Right-LHb, while no signal, either nuclear, or cytoplasmic, is observed in the *Sox1* positive Left-LHb (Fig.3e, 3f; compare Fig.3e1-e2 with Fig.e3-e4). The medial habenula (MHb, *Kctd12b* positive; Supplementary Fig.12a,c,e) also expresses β-catenin at this stage but the signal is excluded from nuclei in all areas examined (Supplementary Fig.12b,d,f, b1-b2,d1-d8). However, an heterogeneity is observed within MHb, with a selective absence of cytoplasmic expression in the anterior left external component of MHb, known to express *ScPde1a* (Supplementary Fig.12b,d; compare Supplementary Fig.12d1-d2 to d3-d8). The restriction of Wnt signaling to the right habenula at stages 29-31 is reminiscent of the one reported in the zebrafish, as a result of a parapineal mediated left repression[24,25]. In the absence of a parapineal in the catshark, we assessed the dependence of this asymmetry on Nodal signaling, by inhibiting the pathway during its window of left restricted activity, shortly after neural tube closure as previously described[18] (Fig.3g,h). While control embryos exhibit the expected restriction of nuclear β-catenin to the lateral right habenula (Right-LHb; Fig.3g,g1-g4), *in ovo* injection of the Nodal/activin antagonist SB-505124 results in an expansion of the signal to the left one (Left-LHb), resulting in a right isomerism (Fig.3h,h1-h4). Taken together, these data highlight an asymmetric, dynamic canonical Wnt activity in the developing habenulae, and they suggest that the marked restriction to

the lateral right habenula observed starting from stage 29 is dependent on the transient left Nodal activity reported in the diencephalon at earlier stages[18].

The elaboration of lateral right neuronal identities (Right-LHb) is dependent on Wnt signaling in the catshark

In order to test the involvement of the right restricted Wnt activity detected in the lateral habenula in the elaboration of neuronal identities, we next inhibited the pathway using *in ovo* injection of the Wnt antagonist IWR-1, a tankyrase inhibitor which stabilizes the β-catenin degradation complex via axin modification[39] (Fig.4, Supplementary Fig.13) and analyzed resulting phenotypes at stage 31. A single injection of the drug at stage 29, results in a right restriction of the territory exhibing a nuclear distribution of β-catenin in the lateral right habenula (compare Fig.4a,a3,a4 and Fig.4g,g3,g4; Supplementary Fig.13a,e). Expression of the two Left-LHb markers tested, *ScSox1* and *ScNtng2*, expands to the right, in the lateral zone devoid of nuclear β-catenin in all embryos injected with the drug (n=6/6), a phenotype never observed in uninjected or control embryos (compare Fig.4b,c,e and Fig.4h,i,k; Supplementary Fig.13b,f). Partial losses of two Right-LHb markers (*ScProx1* and *ScKiss1)* are consistently observed in this Right-LHb subdomain (compare Fig.4d,f and Fig.4j,l; Supplementary Fig.13c,g). In the mouse, no asymmetric habenular expression of *Prox1* has been reported, but expression of the gene in adjacent thalamic territories has been shown to be dependent on *Tcf7l2*, in line with a dependence on Wnt signaling[40]. Another gene expressed in a neighbouring thalamic region, *Rorα*, is submitted to the same regulation in this species. In view of the gene signature similarities between the catshark lateral habenula and mouse thalamic regions adjacent to the habenulae, we analyzed expression of the catshark *Rorα* orthologue in untreated, control and IWR-1 treated embryos. A lateral right-restricted territory of the gene, forming a radial band adjacent to the external part of MHb, is observed in the habenulae of untreated stage 31 embryos (Supplementary Fig.13d3) and it is lost following IWR-1 treatment (compare Supplementary Fig.13d1,d2 with Supplementary Fig.13d1,d2). These data indicate that Wnt signaling is required for the elaboration of right neuronal identities and represses left ones in the catshark lateral right habenula (Fig.4m). In contrast, we never observed perturbations of *ScEnpp2* and *ScPde1a* expressions in the medial habenula in these treatment conditions (Suppl. Fig.14).

The repression of Wnt signaling rescues lateral left neuronal identities in SB-505124 treated embryos

We previously showed that en early abrogation of Nodal/activin signaling, using in ovo injection of the SB-505124 inhibitor during the diencephalic window of left-restricted Nodal activity, induced a

right isomerism habenular phenotype[18]. In order to test whether Wnt inhibition could rescue lateral left (Left-LHb) neuronal identities in these embryos, we conducted conducted double in ovo injections of SB-505124 (stage 16) and IWR-1 (stage 29) and analyzed resulting phenotypes at stage 31 (Fig.5). As expected, in ovo injections of SB-505124 consistently results in a right isomerism (n=5/5), with a symmetric nuclear distribution of β-catenin in both the left and right lateral habenulae as described above (Fig.3h, Fig.5a; Supplementary Fig.15a), a complete loss of lateral left expression for the two Left-LHb markers tested (*ScSox1* and *ScNtng2*: Fig.5c,d,f; Supplementary Fig.15b,c), concomitantly with a lateral left expansion of Right-LHb markers (*ScProx1* and *ScKiss1*: Fig.5b,e,g; Supplementary Fig.15d). Following an additional IWR-1 injection at stage 29 (n=4/4), the symmetry of habenulae is consistently maintained, but the lateral habenulae exhibit non-overlapping territories of right and left-LHb identities, similar to the right habenulae of IWR-1 treated embryos. Compared to SB-505124 treated embryos, nuclear β-catenin becomes undetectable in lateral territories of variable size found both in the left and right habenulae (compare Fig.5h and 5a; Supplementary Fig.15a and 15e). Expression of Left-LHb markers (*ScSox1*, *ScNtng2*) is restored in the corresponding territories (compare Fig.5c,d,f and Fig.5j,k,m; Supplementary Fig.15b,c and 15f,g), while expression of Right-LHb markers (*ScProx1*, *ScKiss1*) is lost (compare Fig.5b,e,g and Fig.5i,l,n; Supplementary Fig.15b,d and 15f,h). Taken together, these data suggest that a repression of Wnt signaling is sufficient to promote a lateral left identity in the absence of Nodal signaling.

Left- and Right-LHb progenitors exit cell cycles prior to stage 29

In the zebrafish, Wnt signaling has been shown to delay neuronal differentiation in the dorsal habenulae, thus contributing to neuronal diversity and asymmetry[25]. In order to address whether the respective timing of progenitor cell cycle exits in the left and right habenulae, we conducted BrdU (5-bromo-2'-deoxyuridine) pulse chase assays starting from early stages of neurogenesis[37]. BrdU incorporation pulses were conducted at stages 26-27 (two stages difficult to distinguish on live embryos), 28 and 29 and the distribution of BrdU labeled cells was analyzed on transverse sections at different organ levels at stage 31 (Fig.6). The assignment of labeled cells to the main habenular subdomains was assessed by comparison to adjacent sections submitted to ISH (Fig. 6). On the right side, the signal maximal intensity is observed along radial bands, which gradually regress from lateral to medial habenula levels at all stages analyzed (Fig.6a2-a8,b2-b8,c2-c8). A negative territory restricted to posterior and lateral-most Right-LHb territories (*ScProx1* positive and *ScKctd12b* negative) is already present following pulses at stages 26-27 (Fig.6a4-a9) and the BrdU signal completely withdraws from Right-LHb, becoming contained within Right-MHb between stages 28 and 29 (compare Fig.6b1-b9 with Fig.6c1-c9). On the left side, a related pattern is

observed, with the presence of lateral and posterior BrdU negative territories after pulses at stages 26-27 (Fig.6a7-a9) and a full withdrawal of BrdU labeled cells from Left-LHb (*ScSox1* positive and *ScKctd12b* positive) between stages 28 and 29 (Fig.6b1-b9 with Fig.6c1-c9). However a major difference is that on the left side, BrdU negative territories span the anterior-most part of both the medial and lateral habenulae following pulses at all stages analyzed, including stages 26-28 (Fig.6a1-a6,b1-b6). Furthermore, the sharp boundary between BrdU positive and negative cells, observed on the right at all pulse stages and all habenula levels, is not observed on the left at anterior to medial organ levels and pulse stages preceding stage 28. Analysis of horizontal sections of stage 31 embryos submitted to BrdU pulses at stages 28, 28+ and 29 confirm and refine these conclusions (Supplementary Fig.16a-b,e-f). BrdU labeled cells become undetectable in both (*ScKctd12b* negative) Left- and Right-LHb by stage 28+, regressing then from external to internal MHb levels (Supplementary Fig.16c-d,e-f; see also the relative position of Fig.6c). These data indicate that at anterior-most organ levels, progenitors of both lateral and medial territories exit cell cycles earlier on the left than on the right (Fig.6d,e).

The distribution of nuclear β-catenin in the lateral/ventral habenulae reflects asymmetry patterns in the lateral/ventral habenulae of gnathostomes

In the catshark, IHC profiles of β-catenin remain highly asymmetric in the habenulae of juveniles, with nuclear signals restricted to the lateral right habenula (Supplementary Fig.17a7,a8,b3,b4,c5,c6). Heterogeneities are also observed in the medial habenula, cytoplasmic signals being selectively absent in its external anterior left component (Supplementary Fig.17a3-a4). In order to test whether the presence of asymmetries in ventral/lateral habenulae correlates with asymmetric distributions of β-catenin across gnathostomes, we conducted IHC analyses of transverse sections from reedfish and spotted gar juveniles, as well as xenopus tadpoles (stage NF-66) (Figure 7). The lungfish was excluded from this analysis as no positive control signal could be obtained in this species. In the reedfish, no nuclear signal could be observed on the left (Fig.7a1,a2). In contrast, most of the right-restricted *EcKiss1* ventral territory contains a high density of positive nuclei (Fig.7a,a3,a4,7b;). In dorsal right *EcKiss1* negative territory, nuclei are generally unlabeled except in a limited lateral area (Fig.7a5,a6). In contrast, in the spotted gar, a nuclear distribution of β-catenin is observed both on the right and on the left, in ventral *LoKiss1* positive territories (Fig.7c,c1,c2,c3,c4,7d). As in the reedfish, dorsal *LoKiss1* negative territories, are heterogeneous, with areas devoid of signal (such as the dorsal-most part of the left dorsal habenula (Fig.7c), while others contain cytoplasm-restricted or nuclear signals (Fig.7c5,c6). In the xenopus, no nuclear signal could be observed either in the dorsal-most *XtKctd* positive domain, or in the complementary *XtSox1*-positive one (Fig.5e,e1,e2,f,f1,f2,f3,f4). However, a significant proportion of positive nuclei

is present in adjacent ventral territories, corresponding to those expressing *XtProx1* (Fig.7f5,f6,f7,f8). In conclusion, right-restricted nuclear accumulations of β-catenin, maintained until advanced stages of differentiation, correlate with the presence of neuronal identity asymmetries in ventral/lateral habenulae.

DISCUSSION

We show here that the catshark habenulae exhibit a highly asymmetric organization, with a majority of asymmetric profiles reported as such for the first time in a vertebrate to our knowledge. Such profiles are detected in both neural progenitors and neuronal territories and in the latter, they concern not only the medial (dorsal in teleosts) subdomain of habenulae as in the zebrafish, but also their lateral subdomain, which in the catshark harbors very different neuronal identities between the left and the right side. This divergence between the two species questions the origin and the mode of evolution of habenular asymmetries across gnathostomes. Focusing on the lateral/ventral subdomain of habenulae, we find that orthologues of selected left-or right-restricted markers share a striking similarity in asymmetry pattern, not only with the elephant shark, a member of holocephalans (which diverged from elasmobranchs about 410 million years ago[41]), but also with a sarcopterygian, the lungfish and an actinopterygian, the reedfish. This pattern contrasts with the bilateral expressions observed in the lateral habenulae and adjacent ventral territories in the xenopus and the mouse, or in the ventral habenulae of the spotted gar and teleosts. While we cannot completely rule out convergent evolution processes to explain the similarities observed between chondrichthyans, dipneusts and polypterids, we favour an alternative, more parsimonious hypothesis, and propose that the asymmetry pattern observed in the catshark lateral habenulae reflects an ancestral trait of jawed vertebrates, independently lost in tetrapods and neopterygians (Fig.8a). In support of this conclusion, the phylogenetic distribution of asymmetries, shared by members of chondrichthyans and of dipneusts and polypterids, respectively outgroups to tetrapods and neopterygians in sarcopterygians and actinopterygians, is very different from, for instance, the punctuated presence/absence pattern of another asymmetric trait recently identified in teleosts[16]. Furthermore, the relative organization of the territories identified appears very similar between the mouse and xenopus on the one hand and within teleosts on the other hand, arguing against a rapid drift of the corresponding molecular architecture in these taxa. Concerning the former two, it is intriguing that in the mouse, several orthologues of catshark Right-LHb markers (*Prox1*, *Rorα*, *Rerg*) are not expressed in the habenulae but rather in the adjacent paraventricular nucleus of thalamus[40]. Similarly, in xenopus, although the precise posterior and ventral boundary of habenulae is difficult to identify due to the absence of marked morphological landmarks, we observed the same relative location of *Prox1* territory, adjacent to *Sox1* expression in the lateral habenulae. Taken

together, these data suggest that ancient regulations of related neuronal identities may be deployed in different, habenular or thalamic, symmetric or asymmetric, territories depending on species.

Which could be the underlying mechanism? In the catshark, our data highlight a role of Wnt signaling in the elaboration of lateral right versus left neuronal identities (Fig.8b). Contrary to the involvement of Wnt signaling in the elaboration of asymmetries in the zebrafish dorsal habenula, the conversion of Right- into Left-LHb neuronal identities observed in the lateral right habenula following Wnt inactivation is unlikely to result from perturbations of the temporal regulation of neurogenesis[25,42] . Our BrdU analyses indeed suggest that Left- and right-LHb progenitors exit cell cycles largely concomitantly and that Right- and Left-LHb precursors are postmitotic at the stage when Wnt inactivations were conducted. However this is reminiscent of the role of *Tcf7l2*, an effector of Wnt signaling required for the refinement of neuronal identities in thalamic nuclei adjacent to the habenula and for the expression of *Prox1* and *Ror*α in postmitotic neurons in the mouse[40,43]. Similarly, the zebrafish orthologue of *Tcf7l2* is required for the specification of *kiss1* expression in the ventral habenula, suggesting a conserved Wnt dependent regulation of this gene between the zebrafish -symmetric-ventral habenulae and the catshark lateral right habenula[23]. Finally, in the absence of functional data in these species, the detection of β-catenin nuclear distributions in the ventral habenulae of the spotted gar, in the right ventral habenulae of the reedfish and in the *Prox1* expressing region adjacent to the lateral habenulae of the xenopus are consistent with a deep conservation of Wnt signaling in the elaboration of neuronal identities, even though the cellular contexts vary across species. We therefore propose that the Wnt dependence of lateral right neuronal identities observed in the catshark reflects an ancient regulation, which controlled asymmetry formation in the lateral habenulae of ancestral jawed vertebrates and which has been deployed in different, bilateral territories of tetrapods and neopterygians.

How these mechanistic transitions could have taken place remains elusive. Despite the different nature of asymmetries between the catshark lateral habenulae and the zebrafish dorsal habenulae, our analysis highlights many mechanistic similarities in their formation. In both cases, a left-sided Wnt repression is essential, even though it is dependent on Nodal signaling in the former and on an interaction with the parapineal in the latter[24]. Whether the left restricted expression of *Sox1* in the catshark habenula, may be involved in this repression, similar to the role of *sox1a* in the zebrafish parapineal[44], is an intriguing possibility in this respect. We also find that Wnt activity is submitted to a highly dynamic regulation in the catshark as in the zebrafish[22,25]. Finally, neurogenesis in the catshark developing habenulae follows a temporal regulation, resulting in the characteristic lateral to medial organization in radial bands observed. Such a temporal regulation, sequentially regulating neuronal identities, connectivity patterns and functional properties, has also been described in the mouse and the zebrafish[7,42,45]. Its asymmetry in the latter results in an advanced differentiation of

dorsal habenula neurons on the left compared to the right in the latter[25], reminiscent of the early differentiation of MHb neurons selectively observed on the left in the catshark. However, whether conserved neuronal identities may be specified under this regulatory control is currently unknown. In favour of this hypothesis, we find that two genes selectively expressed in the mouse lateral medial habenula (*Spon1*,*Trhde*) have a similar expression territory in the early-born external left medial habenula in the catshark (this study, comparisons with profiles in Allen Brain Atlas). This extends to the medial habenulae the similarities observed between the mouse lateral habenulae and the catshark left ones, raising the question of underlying mechanistic conservations. Wnt signaling may be involved since it is responsible for the delayed differentiation of dorsal habebula neurons on the right relative to the left in the zebrafish[25,42]. Taken together, our data suggest the existence of a conserved regulatory logic for the formation of habenular asymmetries across gnathostomes, with a coupling between a conserved temporal regulation of neurogenesis, and its modification by a repression of Wnt signaling, restricted to the left in the ancestral state. Due to its highly dynamic regulation, the latter may be prone to gradual variations in time and space, themselves resulting in asymmetry diversifications. Such variations may in turn lay the ground for major mechanistic transitions, such as the switch between a Nodal dependent left repression of Wnt signaling, as observed in the lamprey and catshark, to a parapineal dependent one, as established in the zebrafish[18].

REFERENCES

1. Matsumoto, M. & Hikosaka, O. Lateral habenula as a source of negative reward signals in dopamine neurons. *Nature* **447**, 1111–1115 (2007).
2. Stamatakis, A. M. & Stuber, G. D. Activation of lateral habenula inputs to the ventral midbrain promotes behavioral avoidance. *Nat Neurosci* **15**, 1105–1107 (2012).
3. Beretta, C. A., Dross, N., Guiterrez-Triana, J. A., Ryu, S. & Carl, M. Habenula circuit development: Past, present, and future. *Frontiers in Neuroscience* **6**, 1–10 (2012).
4. Andalman, A. S. *et al.* Neuronal Dynamics Regulating Brain and Behavioral State Transitions. *Cell* **177**, 970-985.e20 (2019).
5. Amo, R. *et al.* Identification of the zebrafish ventral habenula as a homolog of the mammalian lateral habenula. *The Journal of neuroscience : the official journal of the Society for Neuroscience* **30**, 1566–1574 (2010).
6. Hashikawa, Y. *et al.* Transcriptional and Spatial Resolution of Cell Types in the Mammalian Habenula. *Neuron* **106**, 743-758.e5 (2020).

7. van de Haar, L. L. *et al.* Molecular signatures and cellular diversity during mouse habenula development. *Cell Reports* **40**, 111029 (2022).
8. Pandey, S., Shekhar, K., Regev, A. & Schier, A. F. Comprehensive Identification and Spatial Mapping of Habenular Neuronal Types Using Single-Cell RNA-Seq. *Current Biology* **28**, 1052-1065.e7 (2018).
9. Ahumada-Galleguillos, P. *et al.* Directional asymmetry in the volume of the human habenula. *Brain Struct Funct.* **222**, 1087–1092 (2016).
10. Concha, M. L. & Wilson, S. W. Asymmetry in the epithalamus of vertebrates. *Journal of Anatomy* **199**, 63–84 (2001).
11. Roussigné, M., Blader, P. & Wilson, S. W. Breaking symmetry: The zebrafish as a model for understanding left-right asymmetry in the developing brain. *Developmental Neurobiology* **72**, 269–281 (2012).
12. Facchin, L., Duboué, E. R. & Halpern, M. E. Disruption of Epithalamic Left–Right Asymmetry Increases Anxiety in Zebrafish. *J. Neurosci.* **35**, 15847–15859 (2015).
13. Chen, W. *et al.* Role of Olfactorily Responsive Neurons in the Right Dorsal Habenula–Ventral Interpeduncular Nucleus Pathway in Food-Seeking Behaviors of Larval Zebrafish. *Neuroscience* **404**, 259–267 (2019).
14. Dreosti, E., Vendrell Llopis, N., Carl, M., Yaksi, E. & Wilson, S. W. Left-right asymmetry is required for the habenulae to respond to both visual and olfactory stimuli. *Current Biology* **24**, 440–445 (2014).
15. Duboué, E. R., Hong, E., Eldred, K. C. & Halpern, M. E. Left Habenular Activity Attenuates Fear Responses in Larval Zebrafish. *Current Biology* **27**, 2154-2162.e3 (2017).
16. Michel, L. *et al.* Diversification of habenular organization and asymmetries in teleosts: Insights from the Atlantic salmon and European eel. *Front. Cell Dev. Biol.* **10**, 1015074 (2022).
17. Villalón, A. *et al.* Evolutionary plasticity of habenular asymmetry with a conserved efferent connectivity pattern. *PLoS ONE* **7**, e35329 (2012).
18. Lagadec, R. *et al.* The ancestral role of nodal signalling in breaking L/R symmetry in the vertebrate forebrain. *Nature communications* **6**, 6686 (2015).
19. Gamse, J. T., Thisse, C., Thisse, B. & Halpern, M. E. The parapineal mediates left-right asymmetry in the zebrafish diencephalon. *Development* **130**, 1059–1068 (2003).

20. Gamse, J. T. *et al.* Directional asymmetry of the zebrafish epithalamus guides dorsoventral innervation of the midbrain target. *Development* **132**, 4869–4881 (2005).
21. deCarvalho, T. N. *et al.* Neurtransmitter map of the asymmetric dorsal habenular nuclei of Zebrafish. *Genesis* **52**, 636–655 (2014).
22. Kuan, Y.-S. *et al.* Distinct requirements for Wntless in habenular development. *Developmental Biology* **406**, 117–128 (2015).
23. Beretta, C. A., Dross, N., Bankhead, P. & Carl, M. The ventral habenulae of zebrafish develop in prosomere 2 dependent on Tcf7l2 function. *Neural development* **8**, 19 (2013).
24. Hüsken, U. *et al.* Tcf7l2 is required for left-right asymmetric differentiation of habenular neurons. *Current Biology* **24**, 2217–2227 (2014).
25. Guglielmi, L. *et al.* Temporal control of Wnt signaling is required for habenular neuron diversity and brain asymmetry. *Development* **147**, dev182865 (2020).
26. Coolen, M. *et al.* The dogfish Scyliorhinus canicula: A reference in jawed vertebrates. *Cold Spring Harbor Protocols* **3**, 1–14 (2008).
27. Mayeur, H. *et al.* When Bigger Is Better: 3D RNA Profiling of the Developing Head in the Catshark Scyliorhinus canicula. *Front. Cell Dev. Biol.* **9**, 744982 (2021).
28. Bray, N. L., Pimentel, H., Melsted, P. & Pachter, L. Near-optimal probabilistic RNA-seq quantification. *Nat Biotechnol* **34**, 525–527 (2016).
29. Pimentel, H., Bray, N. L., Puente, S., Melsted, P. & Pachter, L. Differential analysis of RNA-seq incorporating quantification uncertainty. *Nat Methods* **14**, 687–690 (2017).
30. Kamburov, A., Wierling, C., Lehrach, H. & Herwig, R. ConsensusPathDB—a database for integrating human functional interaction networks. *Nucleic Acids Research* **37**, D623–D628 (2009).
31. Kamburov, A. *et al.* ConsensusPathDB: toward a more complete picture of cell biology. *Nucleic Acids Research* **39**, D712–D717 (2011).
32. Ballard, W. W., Mellinger, J. & Lechenault, H. A series of normal stages for development of Scyliorhinus canicula, the lesser spotted dogfish Chondrichthyes: Scyliorhinidae. *Journal of Experimental Zoology* **267**, (1993).
33. Coolen, M. *et al.* Evolution of axis specification mechanisms in Jawed vertebrates: Insights from a chondrichthyan. *PLoS ONE* **2**, e374 (2007).

34. Lauter, G., Söll, I. & Hauptmann, G. Sensitive Whole-Mount Fluorescent In Situ Hybridization in Zebrafish Using Enhanced Tyramide Signal Amplification. in *Brain Development* (ed. Sprecher, S. G.) vol. 1082 175–185 (Humana Press, 2014).
35. Choi, H. M. T. *et al.* Third-generation in situ hybridization chain reaction: Multiplexed, quantitative, sensitive, versatile, robust. *Development (Cambridge)* **145**, (2018).
36. Schwarzkopf, M. *et al.* Hybridization chain reaction enables a unified approach to multiplexed, quantitative, high-resolution immunohistochemistry and *in situ* hybridization. *Development* **148**, dev199847 (2021).
37. Lagadec, R. *et al.* Neurogenetic asymmetries in the catshark developing habenulae: mechanistic and evolutionary implications. *Sci Rep* **8**, 4616 (2018).
38. Kan, L. *et al.* Dual function of Sox1 in telencephalic progenitor cells. *Developmental Biology* **310**, 85–98 (2007).
39. Huang, S.-M. A. *et al.* Tankyrase inhibition stabilizes axin and antagonizes Wnt signalling. *Nature* **461**, 614–620 (2009).
40. Lipiec, M. A. *et al.* TCF7L2 regulates postmitotic differentiation programs and excitability patterns in the thalamus. *Development* dev.190181 (2020) doi:10.1242/dev.190181.
41. Renz, A. J., Meyer, A. & Kuraku, S. Revealing Less Derived Nature of Cartilaginous Fish Genomes with Their Evolutionary Time Scale Inferred with Nuclear Genes. *PLoS ONE* **8**, e66400 (2013).
42. Aizawa, H., Goto, M., Sato, T. & Okamoto, H. Temporally Regulated Asymmetric Neurogenesis Causes Left-Right Difference in the Zebrafish Habenular Structures. *Developmental Cell* **12**, 87–98 (2007).
43. Lee, M. *et al.* Tcf7l2 plays crucial roles in forebrain development through regulation of thalamic and habenular neuron identity and connectivity. *Developmental Biology* **424**, 62–76 (2017).
44. Lekk, I. *et al.* Sox1a mediates the ability of the parapineal to impart habenular left-right asymmetry. *eLife* **8**, e47376 (2019).
45. Fore, S. *et al.* Functional properties of habenular neurons are determined by developmental stage and sequential neurogenesis. *Sci. Adv.* **6**, eaaz3173 (2020).

LEGENDS

Figure 1. The catshark developing habenulae harbor major asymmetries both in lateral and medial habenulae. a Schemes depicting the experimental strategy for the characterization of molecular asymmetries in catshark habenulae (a1) and the resulting 3D organization observed at stage 31 (a2). **b** Schemes showing a lateral view of catshark stage 31 habenulae, with section planes and levels indicated by dotted lines (b1), and the subdomain organization as observed on a transverse section at a medial level of the structure (b2). **c-o** Transverse sections (dorsal to the top of each panel) after ISH with probes for *ScSox1* (f,i), *ScPde1a* (c), *ScKctd12b* (d,g,j), *ScEnpp2* (e), *ScProx1* (h,k), and after fluorescent double ISH with probes for *ScPde1a*/*ScKctd12b* (l), *ScKctd12b*/*ScEnpp2* (m), *ScSox1*/*ScKctd12b* (n) and *ScKctd12b*/*ScProx1* (o). In the latter, signals for *ScKctd12b* are shown in green and those for *ScPde1a*, *ScEnpp2*, *ScSox1* and *ScProx1* are shown in magenta. **p** Scheme showing the subdomain organization of stage 31 habenulae, as observed on a horizontal section at a medial level of the structure. **q-u** Horizontal sections (anterior to the top of each panel) after ISH with probes for *ScSox1* (q), *ScPde1a* (r), *ScKctd12b* (s), *ScEnpp2* (t) and *ScProx1* (u). Sections (c-e), (f-h) and (i-k) were obtained from the same embryo, same for (q-u). Black and white arrowheads respectively point to *ScSox1* and *ScProx1* major lateral territories and asterisks show contra-lateral minor posterior territories. Dotted lines in (c-m,q-u) delimit external and internal subdomains of the medial habenula, as inferred from the inner boundaries of *ScPde1a* and *ScEnpp2* territories. Thin arrows in (c,e,l,m,r,t) point to the boundary between *ScPde1a* and *ScEnpp2* complementary territories in the external MHb subdomain. Color code in (b2): yellow, left-LHb; light purple, MHb; blue, right-LHb. Color code in (a2,p): yellow, left-LHb; light purple, internal MHb; magenta, anterior-left component of external MHb; dark purple, right plus posterior-left components of external MHb. Abbreviations: ant., anterior; post., posterior; ext., external; int., internal; MHb, medial habenula; LHb, lateral habenula; hc, habenular commissure; pi, pineal stalk; L, left; R, right. Scale bar=100μm.

Figure 2. Asymmetries related to those observed in catshark lateral habenulae are detected in dipneusts and polypterids but not neopterygians or tetrapods. a,g,m Schemes depicting the asymmetric organization of the catshark habenulae, with the reference signature markers of left-LHb (a, yellow), MHb (g, purple) and right-LHb (m, blue) considered for cross-species comparisons. **b-f,h-l,n-r** Transverse sections of habenulae in elephant shark (*C. milii*: b,h,n), reedfish (*E. calabaricus*: c,i,o), spotted gar (*L. oculatus*: d,j,p), lungfish (*P. annectens*: e,k,q) and xenopus (*X. tropicalis*: f,l,r) juveniles, following ISH with probes for orthologues of catshark markers for Left-LHb (b-f), MHb (h-l) and Right-LHb (n-r). Dorsal is to the top in all panels and

probe identity is indicated on each view. Black arrowheads in (b-f) point to territories restricted to the left in the elephant shark, the reedfish and the lungfish similar to the catshark, but bilateral in the spotted gar and xenopus. White arrowheads in (n-r) point to territories restricted to the right in the elephant shark, the lungfish and the reedfish as in the catshark, but bilateral in the spotted gar and the xenopus. Black arrows indicate the boundary between dorsal/medial and ventral/lateral habenulae. Dotted lines in (f,l,r) delineate the boundary between the lateral *Sox1* habenular territory and adjacent *Prox1* territory in *X. tropicalis*. **s-w** Schemes depicting territories related to catshark Left-LHb (yellow), MHb (purple) and Right-LHb (blue) in the elephant shark (s), the reedfish (t), the spotted gar (u), the lungfish (v) and the xenopus (w) based on the set of signature markers analyzed. Only markers supporting these relationships are indicated for each species, with those also expressed in additional territories labeled by an asterisk (see expression details in Supplementary Fig.7-11). Abbreviations: same as in Fig.1; dHb, dorsal habenula; vHb, ventral habenula. Scale bar=500µm in (b,h,n), 200µm in (c-d,i-j,o-p), 150µm in (e,k,q), 100µm in (f,l,r).

Figure 3. The nuclear β-catenin profile in the catshark developing habenulae harbors dynamic, Nodal dependent asymmetries. a-f Confocal images of transverse sections of catshark habenulae at stages 26 (a,b), 28 (c), 29 (d) and 31 (e) following DAPI staining (blue) and IHC with antibodies directed against β-catenin (red, a-e) and HuC/D (green, a-b). The section shown in (a) is located anteriorly to the one shown in (b), sections in (c-h) are located at a medial organ level. **f** HCR-FISH image of a section adjacent to (e) with territories for *ScSox1*, *ScKctd12b* and *ScProx1* respectively in yellow, magenta and cyan. White arrowheads in (e,f) point to Right-LHb. Dotted lines in (e,f) delimit LHb and MHb subdomains, respectively positive for *Prox1* and *Kctd12b*. **g-h** Confocal images of transverse sections of stage 31 catshark habenulae following in ovo injection of DMSO (g, control) or SB-505124 (h) following neural tube closure. A white arrowhead in (h) points to a lateral left territory showing a high density of β-catenin positive nuclei as on the right side, present in SB-505124 treated embryos but absent from control ones. **i** Schemes depicting the injection experimental procedure and the habenular phenotypes observed, with lateral territories of nuclear β-catenin accumulation in red. Dorsal is to the top in all panels. Magnifications of boxed areas in (a-e,g-h) are shown in (a1-4 to e1-4,g1-4,h1-4). White arrows point to β-catenin labeled nuclei. Scale bar=100µm.

Figure 4. Inhibition of Wnt signaling converts lateral right into lateral left neuronal identities in the catshark habenulae. a-l Transverse sections of catshark stage 31 habenulae from control (a-f) and IWR-1 treated (g-l) embryos, after IHC with an antibody directed against β-catenin (a,g; β-

catenin in red, DAPI stained nuclei in blue), HCR-FISH with territories of *ScSox1* and *ScProx1* in yellow and cyan respectively (b,h), ISH with probes for *ScSox1* (c,i), *ScProx1* (d,j), *ScNtng2* (e,k) and *ScKiss1* (f,l). Sections are shown at a medial organ level, dorsal to the top. (a) and (b) show adjacent sections of the same embryo, same for (c) and (d), (e) and (f), (g) and (h), (i) and (j), (k) and (l). (a1-a4) and (g1-g4) show magnifications of the territories boxed in (a) and (g), with β-catenin signals in (a1,a3,g1,g3) and DAPI signals in (a2,a4,g2,g4). White arrows point to β-catenin labeled nuclei. Arrowheads in (g-l) show expansions of Left-LHb markers, concomitant with the loss of Right-LHb markers and of nuclear β-catenin accumulation to the lateral right habenula. n in (a-l) refers to the number of embryos exhibiting the same phenotype for the markers and detection method shown. **m** Schemes depicting the experimental procedure used for pharmacological treatments and the resulting habenular phenotypes, with territories of nuclear β-catenin accumulation in red, territories of Left- and Right-LHb identity in yellow and blue respectively. Scale bar=100μm.

Figure 5. Inhibition of Wnt signaling rescues Left-LHb neuronal identities in the lateral habenulae of SB-505124 treated embryos.

a-n Transverse sections of catshark stage 31 habenulae from SB-505124 (a-g) and SB-505124-IWR-1 treated (h-n) embryos, after IHC with an antibody directed against β-catenin (a,h; β-catenin in red, DAPI stained nuclei in blue), HCR-FISH with territories of *ScSox1* and *ScProx1* in yellow and cyan respectively (b,c,i,j), ISH with probes for *ScSox1* (d,k), *ScProx1* (e,l), *ScNtng2* (f,m) and *ScKiss1* (g,n). Sections are shown at a medial organ level, dorsal to the top. (a-c) show sections of the same embryo, same for (d,e), (f,g), (h-j), (k,l) and (m,n). (a1-a2) and (h1-h2) show magnifications of the territories boxed in (a) and (h), with β-catenin signals in red and DAPI signals in blue. A right isomerism is observed following SB-505124 treatment (a-g). Arrowheads in (h-n) point to bilateral LHb sub-territories harboring a Left- LHb identity as a result of the additional IWR-1 treatment. The n number in panels (a-n) refers to the number of embryos exhibiting the same phenotype for the markers and detection method shown. **o** Schemes depicting the experimental procedure used for pharmacological treatments and the resulting habenular phenotypes, with territories of nuclear β-catenin accumulation in red, territories of Left- and Right-LHb identity in yellow and blue respectively. Abbreviations: hc, habenular commissure; L, left; R, right. Scale bar=100μm.

Figure 6. Spatial and temporal regulation of progenitor cycle exits in the catshark developing habenulae. a-d Transverse sections of catshark stage 31 habenulae following exposure of embryos

to BrdU pulses at stage 26-27 (a), 28 (b) and 29 (c), dorsal to the top. (a2,a5,a8,b2,b5,b8,c2,c5,c8) show confocal images following IHC using an antibody directed against BrdU (green; DAPI stained nuclei in gray). (a1,a4,a7,b1,b4,b7,c1,c4,c7), (a3,a6,a9) and (b3,b6,b9,c3,c6,c9) respectively show confocal images after double ISH with probes for *ScKctd12b* (magenta)/*ScProx1* (cyan), *ScSox1* (yellow)/*ScKctd12b* (magenta) and *ScKctd12b* (magenta)/*ScEnpp2* (yellow), with DAPI stained nuclei in gray. (a1,a2,a3) show adjacent sections at an anterior level, same for (b1,b2,b3) and (c1,c2,c3); (a4,a5,a6) show adjacent sections at a medial level, same for (b4,b5,b6) and (c4,c5,c6); (a7,a8,a9) show adjacent sections at a posterior level, same for (b7,b8,b9) and (c7,c8,c9). White dotted lines delimit the border between medial (MHb) and lateral (LHb) territories as inferred from *ScKctd12b* expression, and its approximate location in BrdU labeled sections. Thin arrows point to BrdU negative territories. **d** Scheme showing the spatial distribution of territories exiting cell cycles earlier than stage 27 (1), between stages 27-28 (2), stages 28-28+ (3), stages 28+-29 (4), and later than stage 29 (5), superimposed to the subdomain organization of catshark stage 31 habenulae. **e** Scheme showing the developmental windows when the broad territories of stage 31 catshark habenulae exit cell cycles. Data from Supplementary Figure 16 are taken into account in (e) and (f). Same colour code in (e,f) as in Fig.1p. Scale bar=100μm.

Figure 7. Evolution of nuclear β-catenin asymmetry patterns in the habenulae of jawed vertebrates. a-f Transverse sections of habenulae from reedfish (*E. calabaricus*; a-b), spotted gar (*L. oculatus*; c-d), Western clawed xenopus (*X. tropicalis*; e-f) juveniles after IHC using an antibody directed against β-catenin (red), DAPI stained nuclei in blue;a,c,e) and after ISH with probes for *Kiss1* orthologues (b,d). Dorsal is to the top in all panels. Arrows in (a,b,c,d) indicate the boundary between ventral, *Kiss1* positive territories and dorsal ones. (a1-a6), (c1-c6), (e1-e2) and (f1-f8) show higher magnifications of territories boxed in (a), (c), (e) and (f) respectively, with white arrows pointing to β-catenin positive nuclei. Scale bars=100μm in (a-f).

Figure 8. Evolution of habenular asymmetries in jawed vertebrates. a Distribution of neuronal identity asymmetries in lateral/ventral habenulae across jawed vertebrates. Schemes depict the general subdomain organization of habenulae in eight members of the major gnathostome taxa, with medial/dorsal territories in purple, and lateral/ventral territories in yellow (territories of neuronal identity related to catshark Left-LHb) or blue (territories of neuronal identity related to catshark Right-LHb). The phylogenetic distribution of asymmetries suggests that the neuronal identity asymmetries observed in the catshark lateral habenulae reflect an ancestral trait (node 1 of the tree), maintained in chondrichthyans (node 2) as well as in ancestral actinopterygians (node 3), persisting on the left side in ancestral sarcopterygians (node 5), but independently lost in neopterygians and

tetrapods (nodes 4 and 6). **b** Differential deployment of an ancestral Wnt dependent regulatory module across jawed vertebrates. Together with data available in the mouse and the zebrafish, the functional analysis in the catshark suggests that the Wnt dependence of *Kiss1/Prox1/Rora* expressions observed in the catshark lateral right habenula may reflect an ancient regulatory module, recruited to the patterning of symmetric territories (respectively ventral habenula and dorsal thalamus) in neopterygians and tetrapods.

Supplementary Figure 1. Functional annotation of left- and right-enriched genes identified by transcriptomic analysis. a Scheme showing the pipeline used for the functional annotation of genes identified by the transcriptomic comparison between the left and right catshark habenulae. **b-d** Lists of over-represented GO (Gene Ontology) terms retrieved from both left- and right-enriched gene lists (b), only from the list of left-enriched genes (c) or from the list of right-enriched genes (d). For each term, the corresponding p-value (shaded in yellow for left-enriched genes and in blue for right-enriched ones is indicated. Abbreviation: GPCR, G protein coupled receptor; L, left; R, right.

Supplementary Figure 2. Expression profiles of left- or right-enriched genes showing regionalized ISH profiles in stage 31 catshark habenulae. **a** Schemes showing a lateral view of a stage 31 embryonic brain (a1; habenulae boxed in red), a lateral view of the habenulae with a dotted line indicating the transverse section plane used (a2), and the subdomain organization as observed on a section at a medial level. A dotted line delimits the external and internal components of the medial habenula. Color code: yellow, left-LHB; light purple, MHb; blue, right-LHB; magenta, anterior left external MHb; dark purple, right plus posterior left external MHb; hatched, proliferative pseudo-stratified neuroepithelium. **b-h** transverse sections following ISH with probes for Left-LHb markers (b), anterior left external MHb markers (c)**,** MHb markers (d)**,** right+posterior-left external MHb markers (e), Right-LHb markers (f)**,** genes expressed in combinations of LHb and MHb territories (g) and neural progenitor (LVZ) markers (h). Dorsal is to the top for all sections. For each gene, the rank (r) based on q-value in the list of asymmetrically expressed genes and the laterality of the enrichment is indicated at the bottom left of the panel. Black and white arrowheads in (b,f) respectively point to left- and right-LHb labeled territories, thin arrows in (c,e) point to the boundary between complementary anterior and posterior territories within the left external MHb. Abbreviations: ant., anterior; post., posterior; LVZ, lateral ventricular zone; LHb, lateral habenula; MHb, medial habenula; hc, habenular commissure; L, left; R, right; pi, pineal. Scale bar=100μm.

Supplementary Figure 3. Expression of *ScSox1*, *ScPde1a*, *ScKctd12b*, *ScEnpp2* and *ScProx1* along the antero-posterior axis of stage 31 catshark habenulae. a Schemes showing a lateral view of stage 31 catshark habenulae, with transverse section planes indicated by dotted lines (a1) and their subdomain organization, as observed on a section at a medial level of the structure (a2). Color code: yellow, left-LHB; light purple, internal MHb; blue, right-LHB; magenta, anterior left external MHb; dark purple, right plus posterior left external MHb; hatched, proliferative pseudo-stratified neuroepithelium. **b-f** Transverse sections after ISH with probes for *ScSox1* (b), *ScPde1a* (c), *ScKctd12b* (d), *ScEnpp2* (e) and *ScProx1* (f), dorsal to the top of each panel. All sections shown were obtained from the same embryo. (b1-f1), (b2-f2), (b3-f3), (b4-f4) and (b5-f5) each show successive adjacent sections. (b1-5), (c1-5), (d1-5), (e1-5) and (f1-5) each show sections from anterior to posterior levels as indicated in (a2). Arrowheads point to lateral habenulae, with black and white arrowheads respectively for Left- and Right-Lhb. Asterisks in (b5) and (f4) show *ScSox1* and *ScProx1* posterior minor expression sites, contra-lateral to their main lateral territory. Dotted lines delimit the subdivision of the medial habenula into external and internal components, as inferred from the inner boundaries of *ScPde1a* and *ScEnpp2* territories. Thin black arrows indicate the boundary between *ScPde1a* and *ScEnpp2* complementary territories within the left external medial habenula. Abbreviations: hc, habenular commissure, pi, pineal; LHb lateral habenula; MHb, medial habenula; ext., external; int., internal, L, left;R, right. Scale bar=100µm.

Supplementary Figure 4. Expression of *ScSox1*, *ScPde1a*, *ScKctd12b*, *ScEnpp2* and *ScProx1* along the dorso-ventral axis of stage 31 catshark habenulae. a Schemes showing a lateral view of stage 31 catshark habenulae, with horizontal section planes indicated by dotted lines (a1) and their subdomain organization, as observed on a section at a medial level of the structure (a2). Same color code as in Supplementary Fig.3. **b-f** Horizontal sections after ISH with probes for *ScSox1* (b), *ScPde1a* (c), *ScKctd12b* (d), *ScEnpp2* (e) and *ScProx1* (f), anterior to the top of each panel. All sections shown were obtained from the same embryo. (b1-f1), (b2-f2), (b3-f3) and (b4-f4) each show successive adjacent sections. (b1-4), (c1-4), (d1-4), (e1-4) and (f1-4) each show sections from dorsal to ventral levels as indicated in (a1). Arrowheads point to lateral habenulae, with black and white arrowheads respectively for Left- and Right-LHb. Asterisks in (b4) and (f3) show *ScSox1* and *ScProx1* posterior minor expression sites, contra-lateral to their main lateral territory. Dotted lines delimit the subdivision of the medial habenula into external and internal components, as inferred from the inner boundaries of *ScPde1a* and *ScEnpp2* territories. Thin black arrows indicate the boundary between *ScPde1a* and *ScEnpp2* complementary territories within the left external medial habenula. Same abbreviations as in Supplementary Fig.3. Scale bar=100µm.

Supplementary Figure 5. Subdomain organization of juvenile catshark habenulae. a Schemes showing a lateral view of juvenile catshark habenulae, with section planes used in (b-k) indicated by dotted lines (a1) and their subdomain organization, as observed on a transverse section at an anterior level of the structure (a2). Same color code as in Supplementary Fig.3. **b-f** Transverse sections after ISH with probes for *ScSox1* (b), *ScPde1a* (c), *ScKctd12b* (d), *ScEnpp2* (e) and *ScProx1* (f), dorsal to the top of each panel. (b1-f1), (b2-f2), (b3-f3) and (b4-f4) each show successive adjacent sections. (b1-4), (c1-4), (d1-4), (e1-4), and (f1-4) each show sections from anterior to posterior levels as indicated in (a1). **g-k** Horizontal sections at a medial level of habenulae after ISH with probes for *ScSox1* (g), *ScPde1a* (h), *ScKctd12b* (i), *ScEnpp2* (j) and *ScProx1* (k), anterior to the top of each panel. (g), (h), (i), (j) and (k) show successive adjacent sections at the levels indicated in (a1). **l-p** Transverse sections after ISH with probes for *ScNtng2* (l), *ScPcdh17* (m), *ScKctd12a* (n), *ScKctd8* (o) and *ScKiss1* (p), dorsal to the top of each panel. Sections (b-f) were obtained from the same embryo, same for sections (l-p). Arrowheads point to lateral habenulae, with black and white arrowheads respectively for Left- and Right-LHb. Asterisks in (b1,b2,f3) show *ScSox1* and *ScProx1* posterior minor expression sites, contra-lateral to their main lateral territory. Dotted lines delimit the subdivision of the medial habenula into external and internal components, as inferred from the inner boundaries of *ScPde1a* and *ScEnpp2* territories. Thin black arrows indicate the boundary between complementary anterior and posterior subdomains of the left external medial habenula. Same abbreviations as in Supplementary Fig.3. Scale bar=100μm.

Supplementary Figure 6. Expression of mouse orthologues of catshark Left-LHb, MHb and Right-LHb markers. a-k Images of mouse adult coronal (a-i) or sagittal (j-k) sections following ISH with probes for *Kctd8* (a), *Spon1* (b), *Trhde* (c), *Ntng2* (d), *Pcdh17* (e), *Prkcq* (f), *Rora* (g), *Prox1* (h), *Stxbp6* (i), *Rerg* (j) and *Pde1a* (k) at the level of habenulae. All images were taken from from Allen Brain Atlas. Gene names are shown with the following color code: orthologues of markers of catshark Left-LHb, yellow; external anterior Left-MHb, magenta; MHb, dark purple; Right-LHb, blue. Abbreviations: LHb, lateral habenula; lMHb, lateral medial habenula; vMHb, ventral medial habenula; MHb, medial habenula; PVT, paraventrivular nucleus of thalamus. Scale bar=420μm in (a-i) and 839μm in (j-k).

Supplementary Figure 7. Subdomain organization of habenulae in the elephant shark *C. milii*. a Schemes showing a left lateral view of the elephant shark brain (a1), with the location of habenulae in red and dotted lines indicating transverse section planes at anterior, medial and posterior levels, and a section at a posterior organ level (a2) with the habenular commissure in gray.

b-i Transverse sections of elephant shark juvenile habenulae after ISH with probes for *CmPcdh17* (b), *CmNtng2* (c), *CmSox1* (d), *CmKctd8* (e), *CmKctd12a* (f), *CmKctd12b* (g), *CmKiss1* (h) and *CmProx1* (i), dorsal to the top. All sections were obtained from the same specimen. The level of the sections along the antero-posterior axis is indicated on each panel. Black and white arrowheads point to lateral territories respectively co-expressing *CmPcdh17*/*CmNtng2*/*CmSox1* on the left and *CmKiss1/CmProx1* on the right. Thin arrows indicate their boundary with *CmKctd8/12a/12b* positive, medial habenula territories. Asterisks in (b,h1,h2) indicate medial territories where *CmPcdh17* (b) and *CmKiss1* (h1,h2) are expressed in addition to their major lateral territories. Dotted lines in (e,f,g) delimit two subdomains, respectively positive or negative for *Kctd12a*, within the left medial habenula. Abbreviations: hc, habenular commissure; L, left; R, Right. Scale bar=500μm.

Supplementary Figure 8. Subdomain organization of habenula in the reedfish *E. calabaricus*. **a** Schemes showing a left lateral view of the reedfish brain (a1) with the location of habenulae in red and dotted lines indicating section planes at anterior, medial and posterior levels, and a section at a medial organ level (a2) with tract zones in gray. **b-j** Transverse sections of reedfish juvenile habenulae after ISH with probes for *EcSox1* (b,e1-3), *EcNtng2* (c), *EcPcdh17* (d), *EcKctd12a* (f1-3), *EcKiss1* (g1-3), *EcProx1* (h), *EcKctd8* (i) and *EcKctd12b* (j), dorsal to the top. Sections (b-d) were obtained from the same specimen, same for sections (e-g) and sections (h-j). (e1,f1,g1), (e2,f2,g2) and (e3,f3,g3) respectively show sections at anterior, medial and posterior organ levels. Black and white arrowheads point to ventral territories respectively co-expressing *EcSox1/EcNtng2/EcPcdh17* on the left and expressing *EcKiss1* on the right. Thin arrows indicate their boundary with *EcKctd8/12a* dorsal habenula territories. *EcProx1* expression is restricted to the right but spans both its dorsal and ventral subdomains, except for a minor dorsal territory, labeled by an asterisk (h). Same abbreviations as in Supplementary Figure 6. Scale bar=100μm.

Supplementary Figure 9. Subdomain organization of habenulae in the spotted gar *L. oculatus*. **a** Schemes showing a left lateral view of the spotted gar brain (a1) with the location of habenulae in red and dotted lines indicating section planes at anterior, medial and posterior levels, and a transverse section at a medial organ level (a2) with tract zones in gray. **b-c** Adjacent horizontal sections of habenulae from the same spotted gar juvenile after ISH with probes for *LoPcdh17* (b) and *LoProx1* (c), anterior to the top. **d-k** Transverse sections after ISH with probes for *LoKctd8* (d1-3), *LoKctd12a* (e1-3), *LoKctd12b* (f1-3), *LoKiss1* (g1-3), *LoProx1* (h1-3), *LoSox1* (i1-2), *LoNtng2* (j) and *LoPcdh17* (k1-2), dorsal to the top. Sections (d,e,g) were obtained from the same specimen, same for sections (j,k). (b,c), (d1,e1,f1,g1,h1,i1,i2,j,k1,k2), (d2,e2,f2,g2,h2) and (d3,e3,f3,g3,h3)

respectively show sections at ventral, anterior, medial and posterior organ levels. Black and white arrowheads point to bilateral ventral territories respectively co-expressing *LoSox1/LoNtng2/LoPcdh17* and *LoKiss1/LoProx1*. Thin arrows indicate their boundary with *LoKctd8/12b* dorsal habenula territories. *LoNtng2* expression includes a dorsal territory, labeled by an asterisk in (j), in addition to its ventral one. Dotted lines in (d,e) delimit two subdomains, respectively positive or negative for *Kctd12a*, within the dorsal habenulae. Same abbreviations as in Supplementary Figure 6. Scale bar=100μm.

Supplementary Figure 10. Habenular subdomain organization in the lungfish *P. annectens*. a Schemes showing a left lateral view of the lungfish brain (a1) with the location of habenulae in red and dotted lines indicating section planes at anterior, medial and posterior levels, and a section at a organ medial level (a2) with tract zones in gray. **b-g** Transverse sections of habenulae from lungfish juveniles, after ISH with probes for *PaPcdh17* (b), *PaNtng2* (c), *PaSox1* (d), *PaKctd8* (e), *PaKctd12b* (f), *PaProx* (g), dorsal to the top. (c1,d1,e1,f1,g1), (c2,d2,e2,f2,g2) and (c3,d3,e3,f3,g3) respectively show sections at anterior, medial and posterior organ levels. Black and white arrowheads point to left restricted *PaSox1* and right restricted *PaProx1* lateral territories respectively. Thin arrows indicate their boundaries with *PaKctd8* medial territory. White dotted lines in (d,e) delimit two subdomains, respectively positive or negative for *Kctd12b*, within the *PaKctd8* positive medial habenula. Same abbreviations as in Supplementary Figure 6. Scale bar=100μm.

Supplementary Figure 11. Subdomain organization of habenulae in the Western clawed xenopus *X. tropicalis*. a Schemes showing a left lateral view of the xenopus brain (a1) with the location of habenulae in red and dotted lines indicating section planes at anterior, medial and posterior levels, and a section at a medial organ level (a2) with tract zones in gray. **b-j** Transverse sections of xenopus juvenile habenulae after ISH with probes for *XtSox1* (b,e), *XtNtng2* (c), *XtPcdh17* (d), *XtKctd8* (f,h), *XtKctd12a* (i), *XtKctd12b* (j), *XtProx1* (g), dorsal to the top. Sections (b,c,d) were obtained from the same specimen, same for sections (e,f,g) and sections (h,i,j). (e1,f1,g1,h1,i1,j1), (b1,c1,d1,e2,f2,g2) and (b2,c2,d2,e3,f3,g3,h2,i2,j2) respectively show sections at anterior, medial and posterior organ levels. Black and white arrowheads respectively point to a bilateral lateral habenula territory co-expressing *XtSox1/XtNtng2* (but not *XtPcdh17*), and an adjacent one expressing *XtProx1*, excluded from anterior-most levels. Thin arrows indicate the medial/dorsal boundary of the former with *XtKctd8/12b* medial habenula territories. At medial to posterior levels, *XtSox1* expression expands to a posterior *XtPcdh17/XtProx1* positive thalamic territory, labeled by an asterisk in (b2,d1,d2,e3,g2,g3), in addition to its habenular one. Dotted lines

in (b,c,e,g) delineate the boundary between these *XtSox1/XtNtng2* and *XtProx1* territories. Dashed lines in (h1,j1) delimit two anterior subdomains, respectively expressing *XtKctd8 and XtKctd12b*, within the medial habenulae. Same abbreviations as in Supplementary Figure 6. Scale bar=50µm.

Supplementary Figure 12. Heterogeneity of β-catenin signal in the catshark medial habenula at stage 31. a-f Confocal images of transverse sections of catshark developing habenulae (stage 31) after HCR-FISH with signals for *ScSox1*, *ScKctd12b* and *ScProx1* in respectively yellow, magenta and cyan (a,c,e), and after IHC using an antibody directed against β-catenin (b,d,f; red). DAPI stained nuclei are shown in blue. All sections were obtained from the same embryo. (a,b), (c,d) and (e,f) each show adjacent sections, at anterior, medial and posterior levels respectively. (b1-2), (d1-8) and (f1-2) show magnifications of the territories boxed in (b), (d) and (f), with β-catenin signals in (b1,d1,d3,d5,d7,f1) and DAPI signals in (b2,d2,d4,d6,d8,f2). White arrowheads and opened arrowheads point to Left- and Right-LHb, an asterisk in (e) marks a minor *ScProx1* right territory. Thin white arrows in (f1-2) point to β-catenin labeled nuclei. A dotted line in (d) delimits a medial territory devoid of cytoplasmic signal for β-catenin (d1,d2), similar to the anterior left habenula (b). These territories correspond by their location to the *ScPde1a/ScKctd12a* expressing MHb sub-territory. A cytoplasmic (but not nuclear) β-catenin signal is observed in all other MHb territories examined (b1-2;d3-8). Abbreviations: hc, habenular commissure; L, left; R, right. Scale bars=100µm.

Supplementary Figure 13. Habenular phenotypes observed along the antero-posterior axis of catshark stage 31 habenulae following IWR-1 treatment. a-l Transverse sections of catshark stage 31 habenulae from control (a-d) and IWR-1 treated (e-h) embryos, after IHC with an antibody directed against β-catenin (a,e; β-catenin in red, DAPI stained nuclei in blue), and ISH with probes for *ScSox1* (b,f), *ScProx1* (c,g), *ScRorα* (d,h),. Section levels along the antero-posterior axis are indicated at the bottom of each panel (a1-g1, anterior; a2-g2,d1,d3,h1, medial: a3-g3,d2,h2, posterior), dorsal is to the top. (b,c) were obtained from the same embryo, same for (f,g). (b1,c1) are adjacent sections, same for (b2,c2), (b3,c3), (f1,g1), (f2,g2) and (f3,g3). (a1',a1"), (a2',a2"), (a3',a3"), (e1',e1"), (e2',e2"), (e3',e3") show magnifications of the territories boxed in (a1), (a2), (a3), (e1),(e2), (e3) respectively, with β-catenin signals in (a1',a2',a3',e1',e2',e3') and DAPI signals in (a1",a2",a3",e1"e2",e3"). Arrowheads in (e-g) show a loss of nuclear β-catenin accumulation in the lateral right habenula (e) and an expansion of *ScSox1* expression to this territory, concomitant with a loss of *ScProx1* expression. Asterisks in (d1,d2) indicate lateral right-restricted territory lost in IWR-1 treated embryo (h1,h2). Scale bar=100µm.

Supplementary Figure 14. IWR-1 treatment at stage 29 has no effect on *ScPde1a* and *ScEnpp2* expression. a-d Transverse sections of catshark stage 31 habenulae from control (a-b) and IWR-1 treated (c-d) embryos, after ISH with probes for *ScPde1a* (a,c) and *ScEnpp2* (b,d). Sections (a1 to a4), (b1 to b4), (c1 to c4) and (d1 to d4) are located from anterior to posterior levels of the habenulae, dorsal is to the top. (a,b) are adjacent sections from the same embryo, same for (c,d). (a1,b1) are adjacent sections, same for (a2,b2), (a3,b3), (a4,b4), (c1,d1), (c2,d2), (c3,d3) and (c4,d4). Dotted lines delimit internal and external components of the medial habenula, a thin arrow points to the boundary between *ScPde1a* and *ScEnpp2* complementary territories in the left external medial habenula. Black and white arrowheads show the location of left and right lateral habenulae respectively. Abbreviations: L, left; R, right. Scale bar=100µm.

Supplementary Figure 15. Habenular phenotypes observed along the antero-posterior axis of catshark stage 31 habenulae following double SB-505124 and IWR-1 treatment. a-l Transverse sections of catshark stage 31 habenulae from SB-505124 (a-c) and double SB-505124/IWR-1 treated (e-g) embryos, after IHC with an antibody directed against β-catenin (a,e; β-catenin in magenta, DAPI stained nuclei in blue), and ISH with probes for *ScSox1* (b,f), *ScProx1* (c,g). Section levels along the antero-posterior axis are indicated at the bottom of each panel (a1-g1, anterior; a1-g2, medial: a3-g3, posterior), dorsal is to the top. (b,c) were obtained from the same embryo, same for (f,g). (b1,c1) are adjacent sections, same for (b2,c2), (b3,c3), (f1,g1), (f2,g2) and (f3,g3). (a1',a1"), (a2',a2"), (a3',a3"), (e1',e1"), (e2',e2"), (e3',e3") show magnifications of the territories boxed in (a1), (a2), (a3), (e1),(e2), (e3) respectively, with β-catenin signals in (a1',a2',a3',e1',e2',e3') and DAPI signals in (a1",a2",a3",e1"e2",e3"). A right isomerism is observed at all axial levels in SB-505124 treayed embryos (a-c). Arrowheads in (e) show bilateral losses of nuclear β-catenin accumulation (e) and bilateral *ScSox1* expressions, concomitant with losses of *ScProx1* expressions (f,g), in subdomains of the lateral habenulae observed in double SB-505124/IWR-1 treated embryos but not in SB-505124 treated ones. **d,h** Schemes depicting the habenular phenotypes observed in SB-505124 (d) and-505124/IWR-1 treated (h) embryos, with territories of nuclear β-catenin accumulation in red, territories of Left- and Right-LHb identity in yellow and blue respectively, and an arrowhead pointing to the territories recovering a lateral left identity in double SB-505124/IWR-1 treated embryos. Scale bar=100µm.

Supplementary Figure 16. Spatial and temporal regulation of progenitor cycle exits in the catshark developing habenulae. a-f Horizontal sections of catshark stage 31 habenulae following exposure of embryos to BrdU pulses at stage 28 (a,b), 28+ (c,d) and 29 (e,f), anterior to the top.

(a,c,e) show confocal images following IHC using an antibody directed against BrdU (green; DAPI stained nuclei in gray). (b,d,f) respectively show confocal images after double ISH with probes for *ScKctd12b* (magenta) and *ScProx1* (cyan), with DAPI stained nuclei in gray. (a1,b1), (a2,b2), (a3,b3) each show adjacent sections of the same embryo at anterior, medial and posterior levels respectively; same for (c1,d1), (c2,d2), (c3,d3) and (e1,f1), (e2,f2), (e3,f3). White dotted lines delimit the border between medial (MHb) and lateral (LHb) territories as inferred from *ScKctd12b* expression, and its approximate location in BrdU labeled sections. Thin arrows point to BrdU negative territories. Scale bar=100µm.

Supplementary Figure 17. Asymmetric β-catenin signals persist in the habenulae of catshark juveniles. a-c Confocal images of transverse sections of catshark juvenile habenulae after IHC using an antibody directed against β-catenin, dorsal to the top. DAPI stained nuclei are shown in blue. All sections were obtained from the same embryo. (a1-8), (b1-4) and (c1-6) show magnifications of the territories boxed in (a), (b) and (c), with DAPI signals in (a1,a3,a5,a7,b1,b3,c1,c3,c5) and DAPI/β-catenin signals in (a2,a4,a6,a8,b2,b4,c2,c4,c6). White arrowheads and black arrowheads point to Left- and Right-LHb. Abbreviations: L, left; R, right. Scale bars=100µm.

Source data

Supplementary Table 1. Transcriptomic analysis of habenular asymmetries in the catshark stage 31 habenulae. Sheet 1 List of differentially expressed genes between the left and the right habenula sides. Differentially expressed gene models are listed in column A, with left- and right-enriched ones shaded in yellow and blue respectively. Curated annotation and automated annotation against Swissprot are indicated in columns B and C. P-values, q-values and fold changes (FC) are given in columns D, E and G. Genes previously identified as left-enriched in the catshark developing habenulae (Lagadec et al, 2015. *Nature com.* 6, 6686) such as *ScPitx2* and *ScKctd12b,* are present in this list. **Sheet 2** Functional annotation of left- and right enriched genes. GO (gene ontology) terms for biological processes over-represented in the lists of left- and right-enriched genes are represented in columns (B,C) and (G,H) respectively, with the corresponding q-values in A and F and the identity of genes taken into account in D and I. Terms are grouped together by level (2 to 5). Those retrieved both for left- and right enriched genes are shown in red characters.

Supplementary Table 2. List of genes analyzed by ISH in the catshark *S. canicula* (sheet 1), the elephant shark *C. milii*, reedfish *E. calabaricus*, spotted gar *L. oculatus*, lungfish *P. annectens* and Western clawed frog *X. tropicalis* (sheets 2-6 respectively). Sheet 1 The genes shown were retrieved from the transcriptomic comparison between stage 31 left and right habenulae except for *ScKctd8*, *ScKctd12a* and *ScRorα*, selected by candidate gene approaches as described in Results. Gene names are indicated in column A, the corresponding identification in the reference database in column B, the laterality of the enrichment predicted by the transcriptomic analysis in column C, the rank in the list of differentially expressed genes in column D (ranking on increasing p-values), the corresponding expression characteristics in column E and the sequence of the probe in column F. Colors indicate the expression characteristics of genes exhibiting regionalized ISH in profiles in differentiated habenula territories with the following code: yellow, Left-LHb; light purple, internal MHb; dark purple, external MHB, right and posterior-left; magenta, external MHB, anterior-left; blue, Right-LHb). Genes expressed in combinations of these domains are shaded in grey. **Sheet 2-6** Columns A, B and C respectively contain gene names, their NCBI identifier and probe sequences.

Supplementary Table 3. Expression characteristics of mouse and zebrafish orthologues of catshark Left-LHb, External anterior Left-MHb, MHB, and Right-LHb markers. References cited: Gamse et al. 2003. Development 130:1059-1068; Gamse et al. 2005. Development 132:4869-48881; Heuer et al. 1998. Eur. J. Neurosci. 10:1465; Kan et al. 2004. Dev Biol. 269:580-94; Lipiec et al. Development 147:dev190181; Nakashiba et al. 2002. Mech Dev. 2002. 111:47-60; O'Dowd et

al. 2000.Mol. Endocrin. 14:183; Pandey et al. 2018. Curr Biol. 8:1052-1065.e7; Van de Haar et al. 2022. Cell Reports 40:111029; Yaguchi et al.2014. Mol Brain 19;7:19.

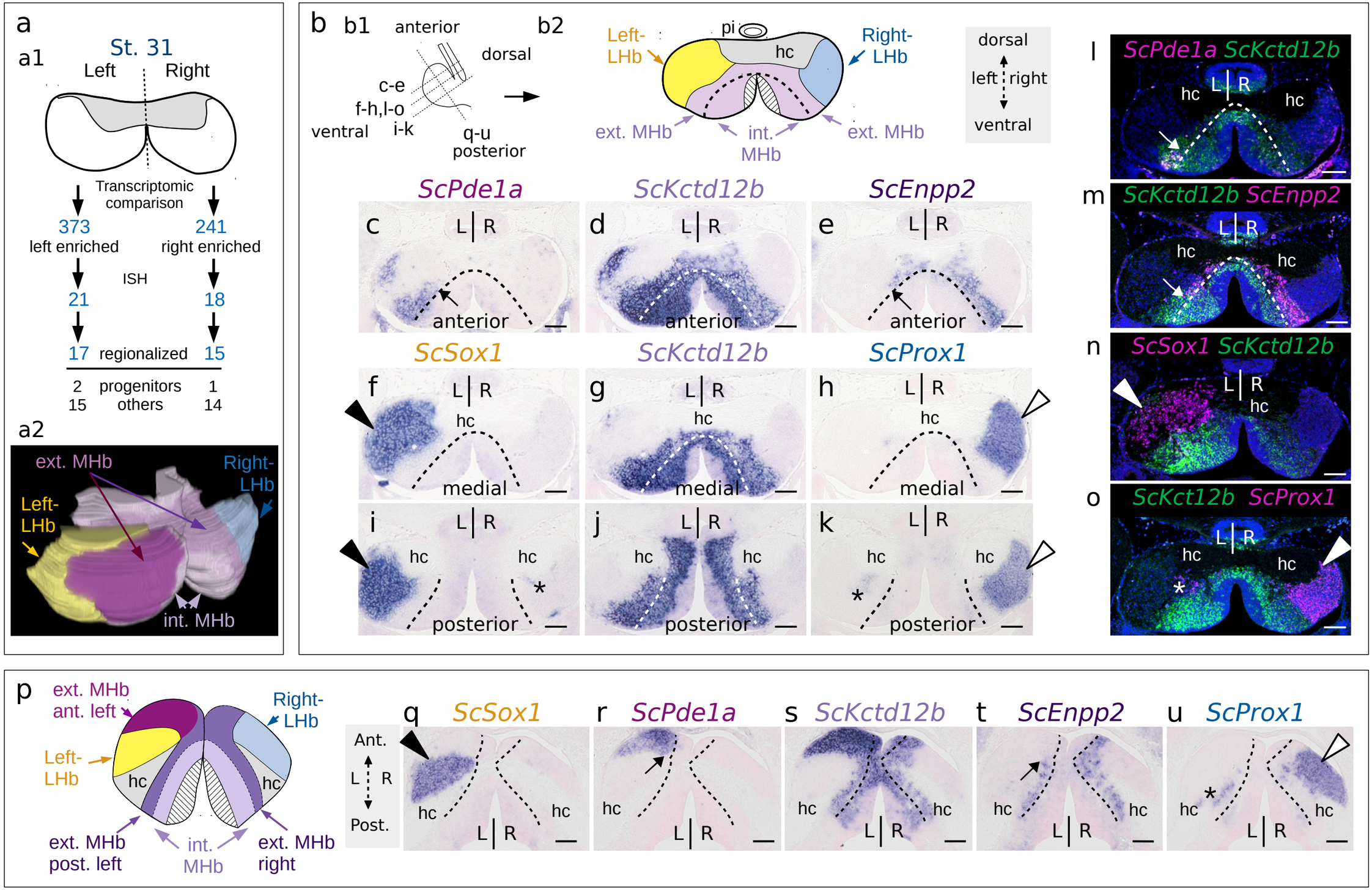
a
a1
St. 31
Left
Right
Transcriptomic comparison
373
left enriched
241
right enriched
ISH
21
18
17 regionalized 15
2 progenitors 1
15 others 14
a2
ext. MHb
Right-LHb
Left-LHb
int. MHb
b
b1
anterior
dorsal
c-e
f-h,l-o
ventral
i-k
q-u
posterior
b2
pi
hc
Left-LHb
Right-LHb
ext. MHb
int. MHb
ext. MHb
dorsal
left right
ventral
ScPde1a
ScKctd12b
ScEnpp2
c
d
e
L R
anterior
ScSox1
ScKctd12b
ScProx1
f
g
h
hc
medial
i
j
k
posterior
l
ScPde1a ScKctd12b
m
ScKctd12b ScEnpp2
n
ScSox1 ScKctd12b
o
ScKct12b ScProx1
p
ext. MHb ant. left
Right-LHb
Left-LHb
hc
ext. MHb post. left
int. MHb
ext. MHb right
Ant.
L R
Post.
q ScSox1
r ScPde1a
s ScKctd12b
t ScEnpp2
u ScProx1

Figure 1

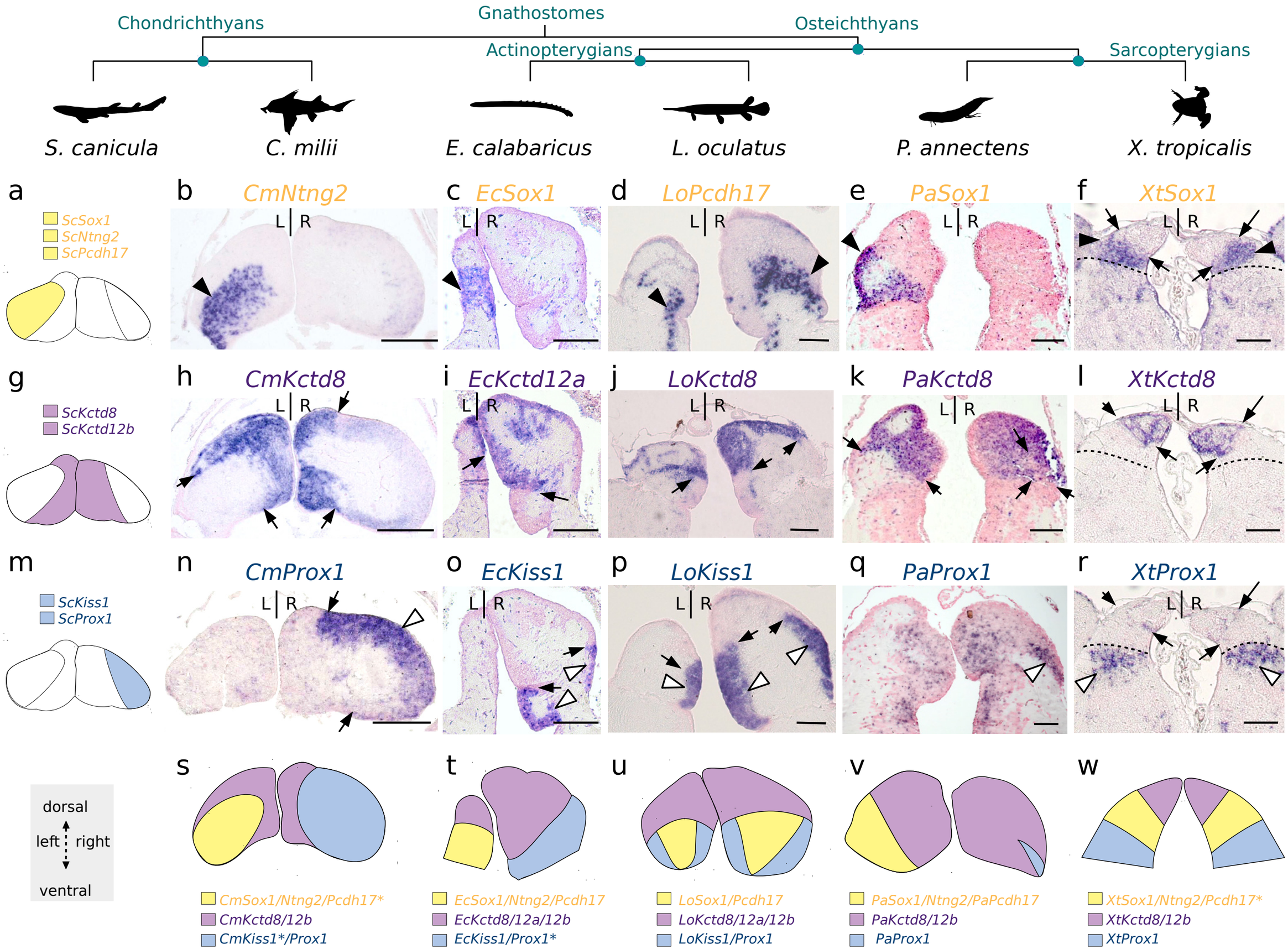
Chondrichthyans
Gnathostomes
Osteichthyans
Actinopterygians
Sarcopterygians
S. canicula
C. milii
E. calabaricus
L. oculatus
P. annectens
X. tropicalis
a
ScSox1
ScNtng2
ScPcdh17
b CmNtng2
c EcSox1
d LoPcdh17
e PaSox1
f XtSox1
g
ScKctd8
ScKctd12b
h CmKctd8
i EcKctd12a
j LoKctd8
k PaKctd8
l XtKctd8
m
ScKiss1
ScProx1
n CmProx1
o EcKiss1
p LoKiss1
q PaProx1
r XtProx1
L R
dorsal
left
right
ventral
s
t
u
v
w
CmSox1/Ntng2/Pcdh17*
CmKctd8/12b
CmKiss1*/Prox1
EcSox1/Ntng2/Pcdh17
EcKctd8/12a/12b
EcKiss1/Prox1*
LoSox1/Pcdh17
LoKctd8/12a/12b
LoKiss1/Prox1
PaSox1/Ntng2/PaPcdh17
PaKctd8/12b
PaProx1
XtSox1/Ntng2/Pcdh17*
XtKctd8/12b
XtProx1

Figure 2

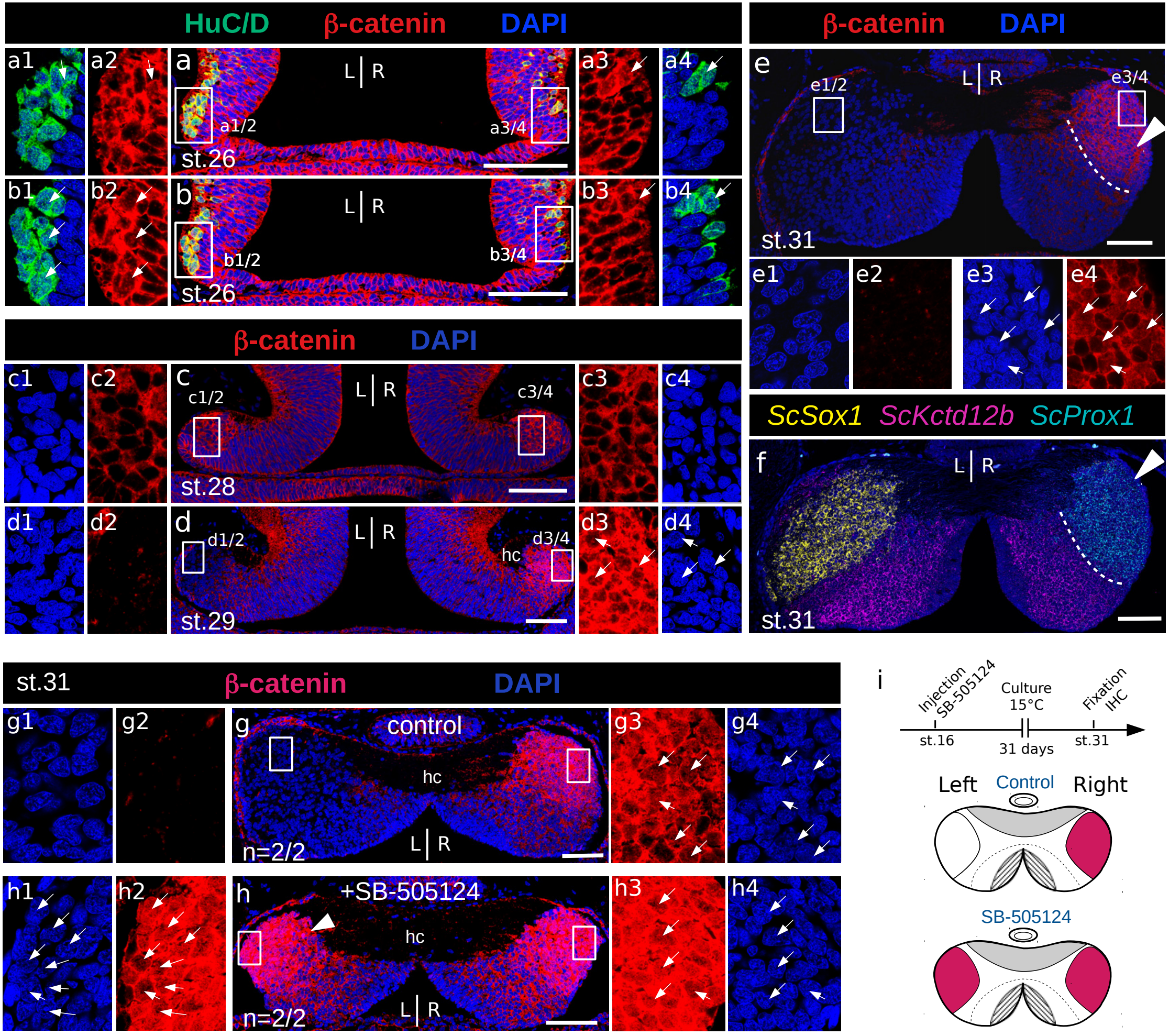
HuC/D β-catenin DAPI
a1
a2
a
L R
a1/2
a3/4
st.26
a3
a4
b1
b2
b
L R
b1/2
b3/4
st.26
b3
b4
β-catenin DAPI
c1
c2
c
c1/2
L R
c3/4
st.28
c3
c4
d1
d2
d
d1/2
L R
d3/4
hc
st.29
d3
d4
β-catenin DAPI
e
e1/2
L R
e3/4
st.31
e1
e2
e3
e4
ScSox1 ScKctd12b ScProx1
f
L R
st.31
st.31 β-catenin DAPI
g1
g2
g
control
hc
n=2/2
L R
g3
g4
h1
h2
h
+SB-505124
hc
n=2/2
L R
h3
h4
i
Injection SB-505124
Culture 15°C
Fixation IHC
st.16
31 days
st.31
Left
Control
Right
SB-505124

Figure 3

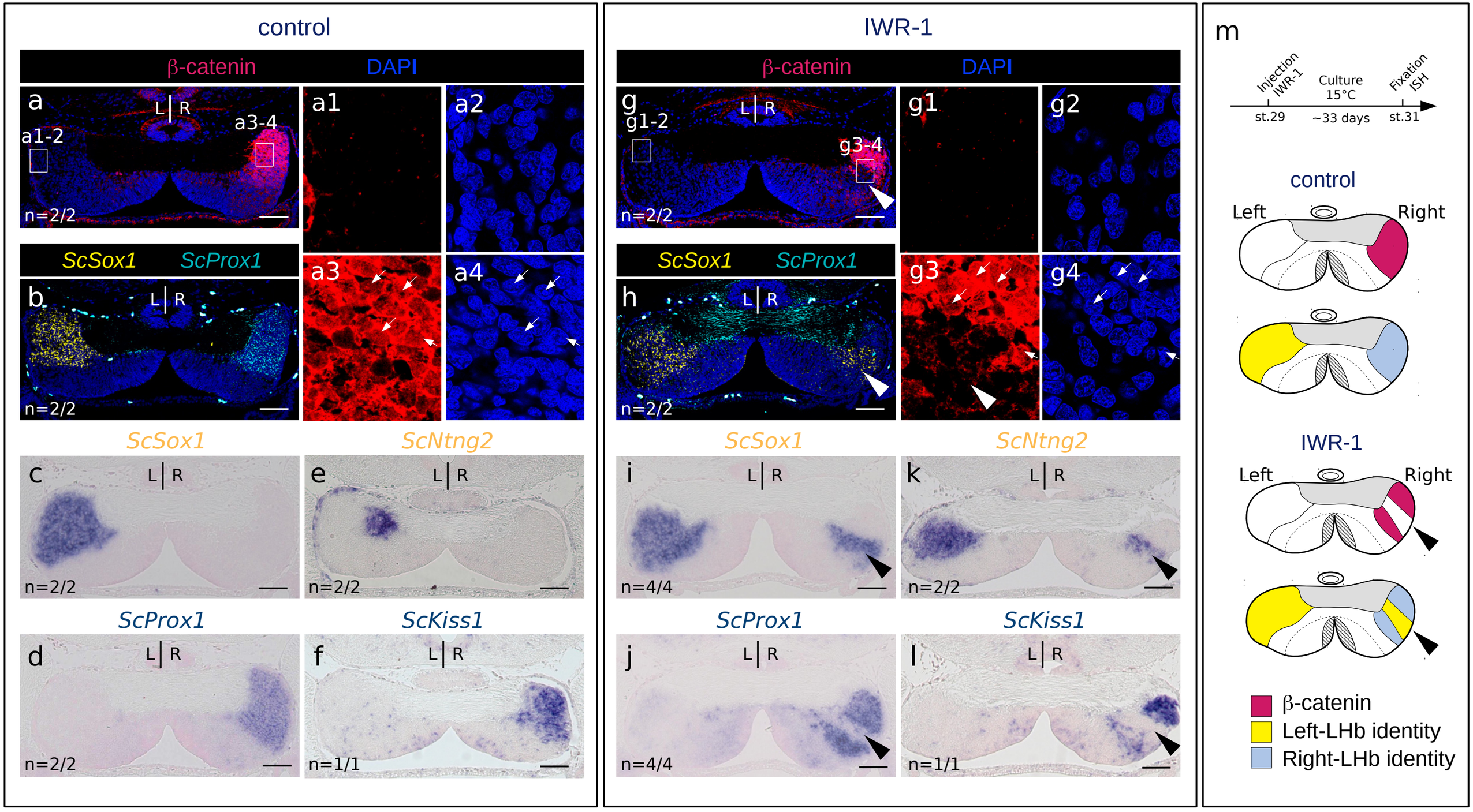
control
β-catenin
DAPI
a
L R
a1-2
a3-4
n=2/2
a1
a2
ScSox1
ScProx1
b
L R
n=2/2
a3
a4
ScSox1
ScNtng2
c
L R
n=2/2
e
L R
n=2/2
ScProx1
ScKiss1
d
L R
n=2/2
f
L R
n=1/1
IWR-1
β-catenin
DAPI
g
g1-2
L R
g3-4
n=2/2
g1
g2
ScSox1
ScProx1
h
L R
n=2/2
g3
g4
ScSox1
ScNtng2
i
L R
n=4/4
k
L R
n=2/2
ScProx1
ScKiss1
j
L R
n=4/4
l
L R
n=1/1
m
Injection IWR-1
Culture 15°C
Fixation ISH
st.29
~33 days
st.31
control
Left
Right
IWR-1
Left
Right
β-catenin
Left-LHb identity
Right-LHb identity

Figure 4

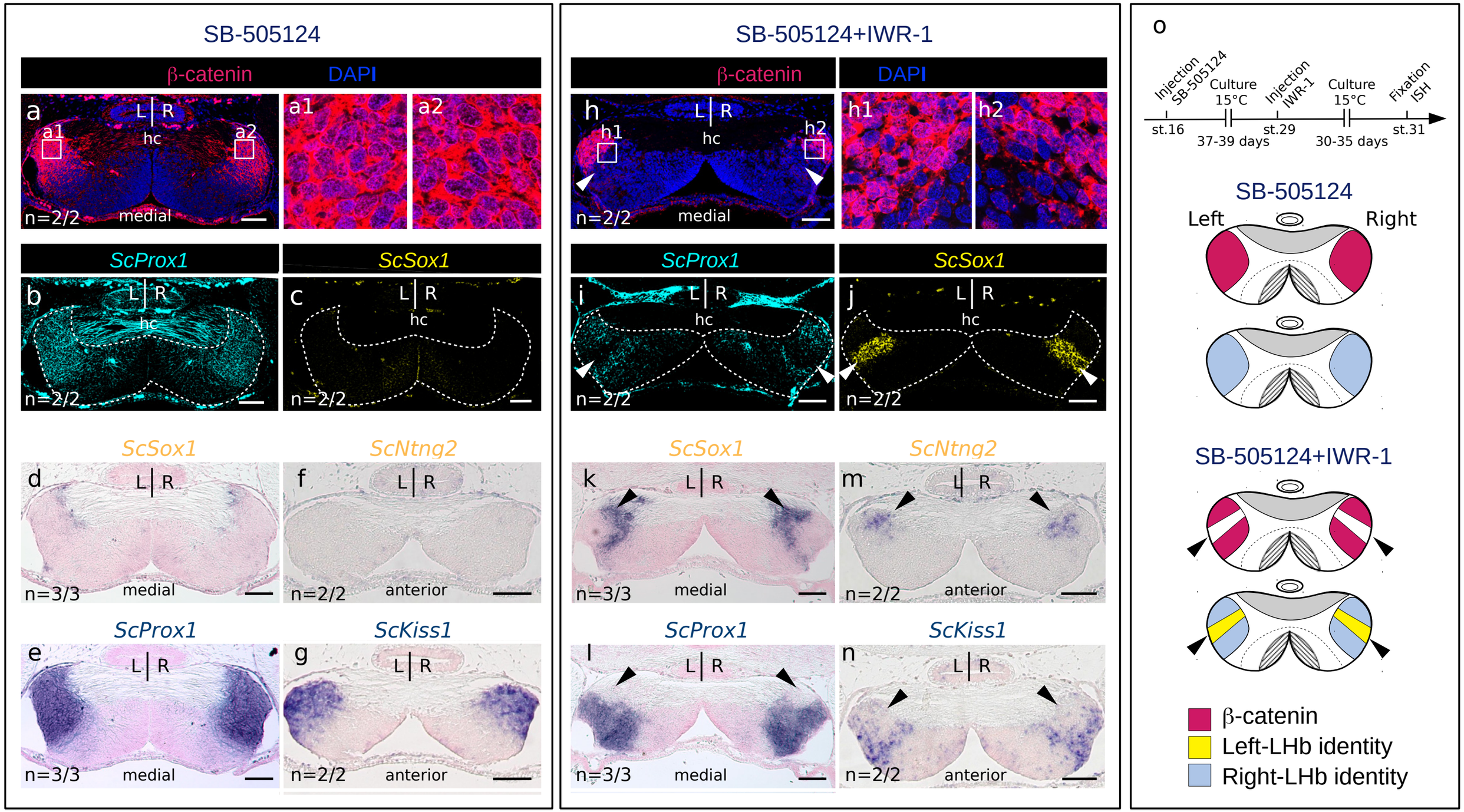
SB-505124
β-catenin
DAPI
a
L R
hc
a1
a2
n=2/2
medial
ScProx1
ScSox1
b
c
n=2/2
ScSox1
ScNtng2
d
f
n=3/3
medial
n=2/2
anterior
ScProx1
ScKiss1
e
g
n=3/3
medial
n=2/2
anterior
SB-505124+IWR-1
h
h1
h2
i
j
k
m
l
n
o
Injection SB-505124
Culture 15°C
Injection IWR-1
Culture 15°C
Fixation ISH
st.16
st.29
st.31
37-39 days
30-35 days
Left
Right
β-catenin
Left-LHb identity
Right-LHb identity

Figure 5

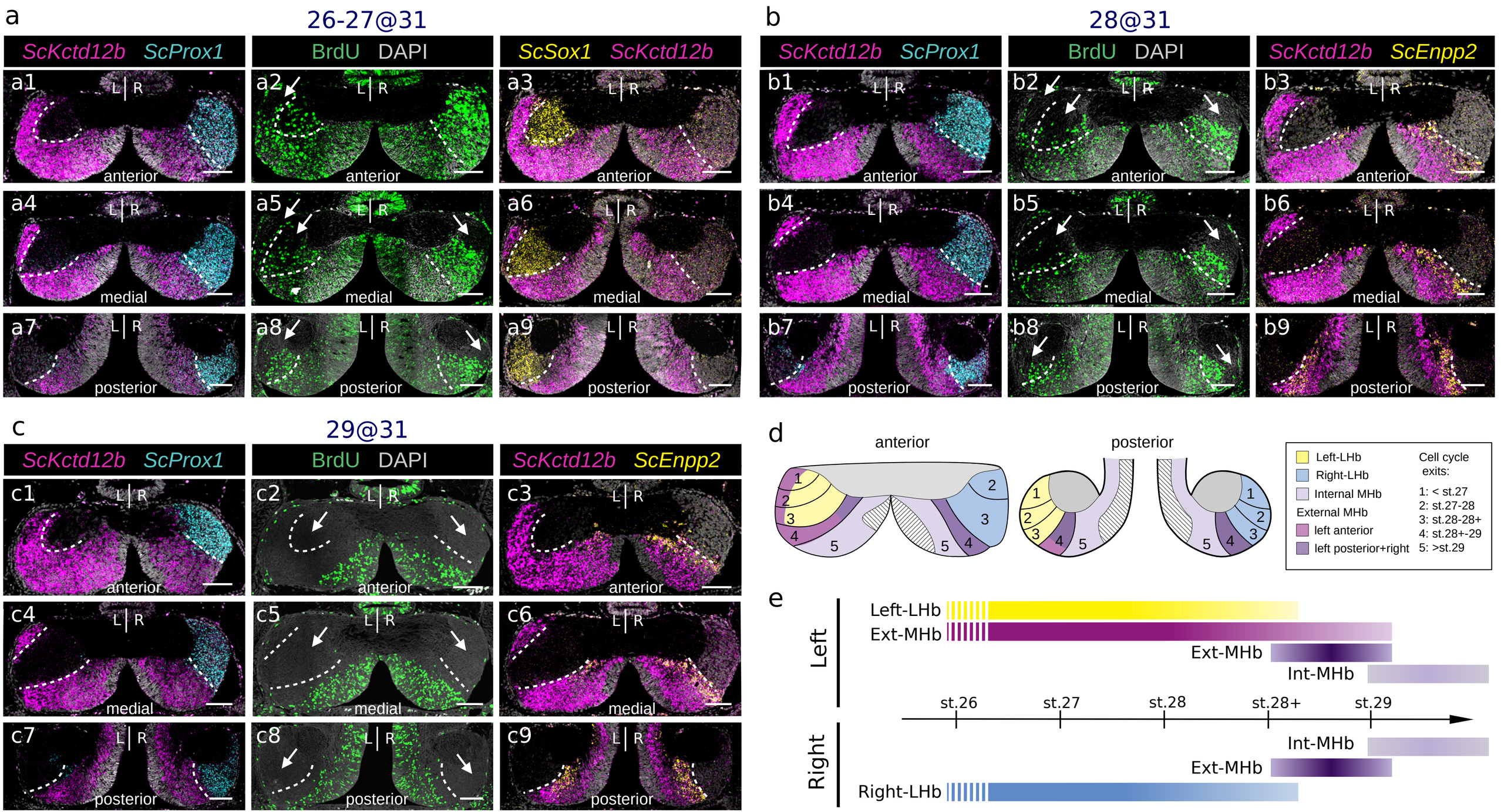
a
26-27@31
ScKctd12b ScProx1
BrdU DAPI
ScSox1 ScKctd12b
a1
a2
a3
a4
a5
a6
a7
a8
a9
L | R
anterior
medial
posterior
b
28@31
ScKctd12b ScProx1
BrdU DAPI
ScKctd12b ScEnpp2
b1
b2
b3
b4
b5
b6
b7
b8
b9
c
29@31
ScKctd12b ScProx1
BrdU DAPI
ScKctd12b ScEnpp2
c1
c2
c3
c4
c5
c6
c7
c8
c9
d
anterior
posterior
Left-LHb
Right-LHb
Internal MHb
External MHb
left anterior
left posterior+right
Cell cycle exits:
1: < st.27
2: st.27-28
3: st.28-28+
4: st.28+-29
5: >st.29
e
Left
Right
Left-LHb
Ext-MHb
Int-MHb
Right-LHb
st.26
st.27
st.28
st.28+
st.29

Figure 6

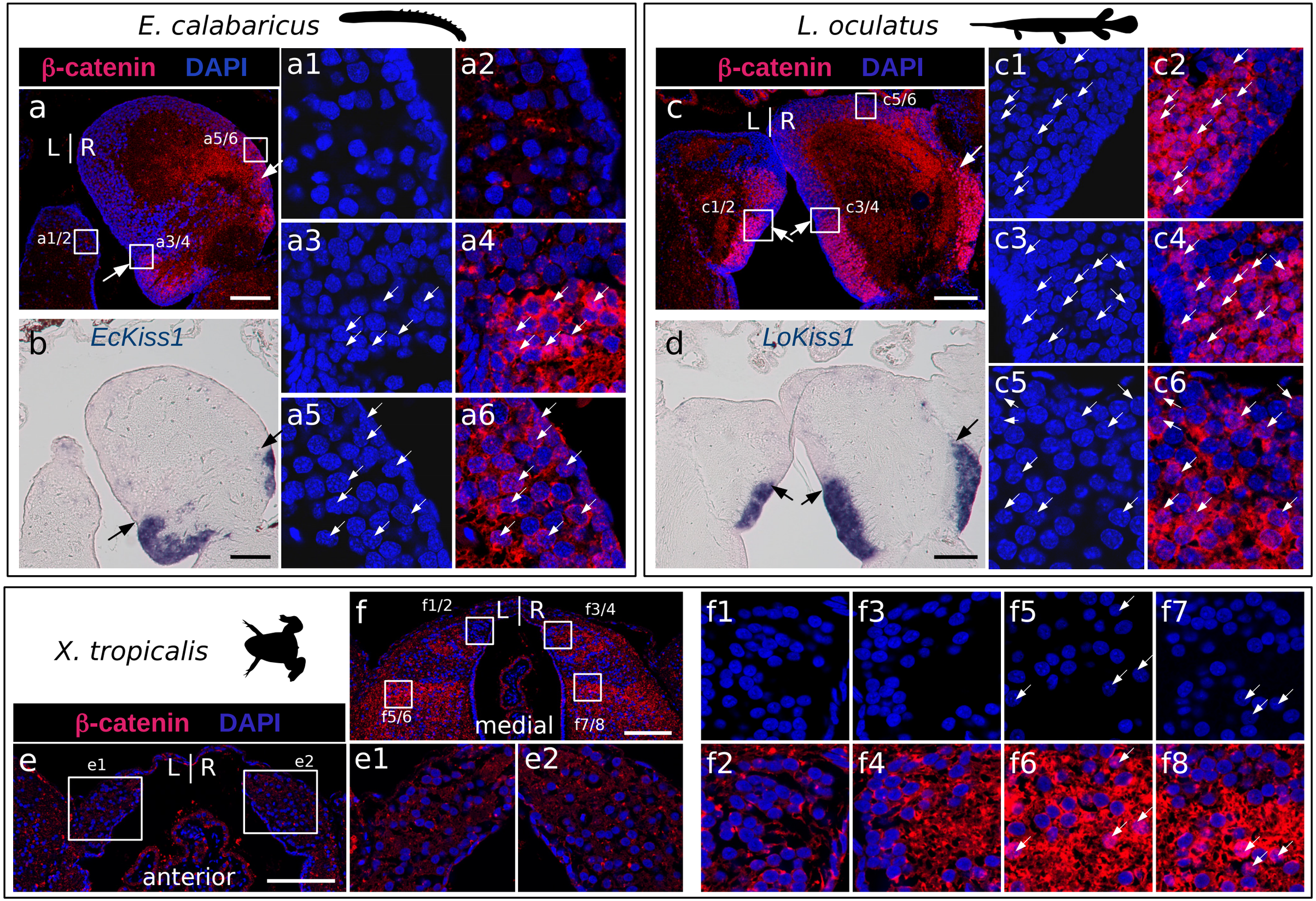
E. calabaricus
β-catenin DAPI
a
L R
a5/6
a1/2
a3/4
a1
a2
a3
a4
a5
a6
b
EcKiss1
L. oculatus
β-catenin DAPI
c
L R
c5/6
c1/2
c3/4
c1
c2
c3
c4
c5
c6
d
LoKiss1
X. tropicalis
β-catenin DAPI
f
f1/2
L R
f3/4
f5/6
medial
f7/8
f1
f3
f5
f7
f2
f4
f6
f8
e
e1
L R
e2
anterior
e1
e2

Figure 7

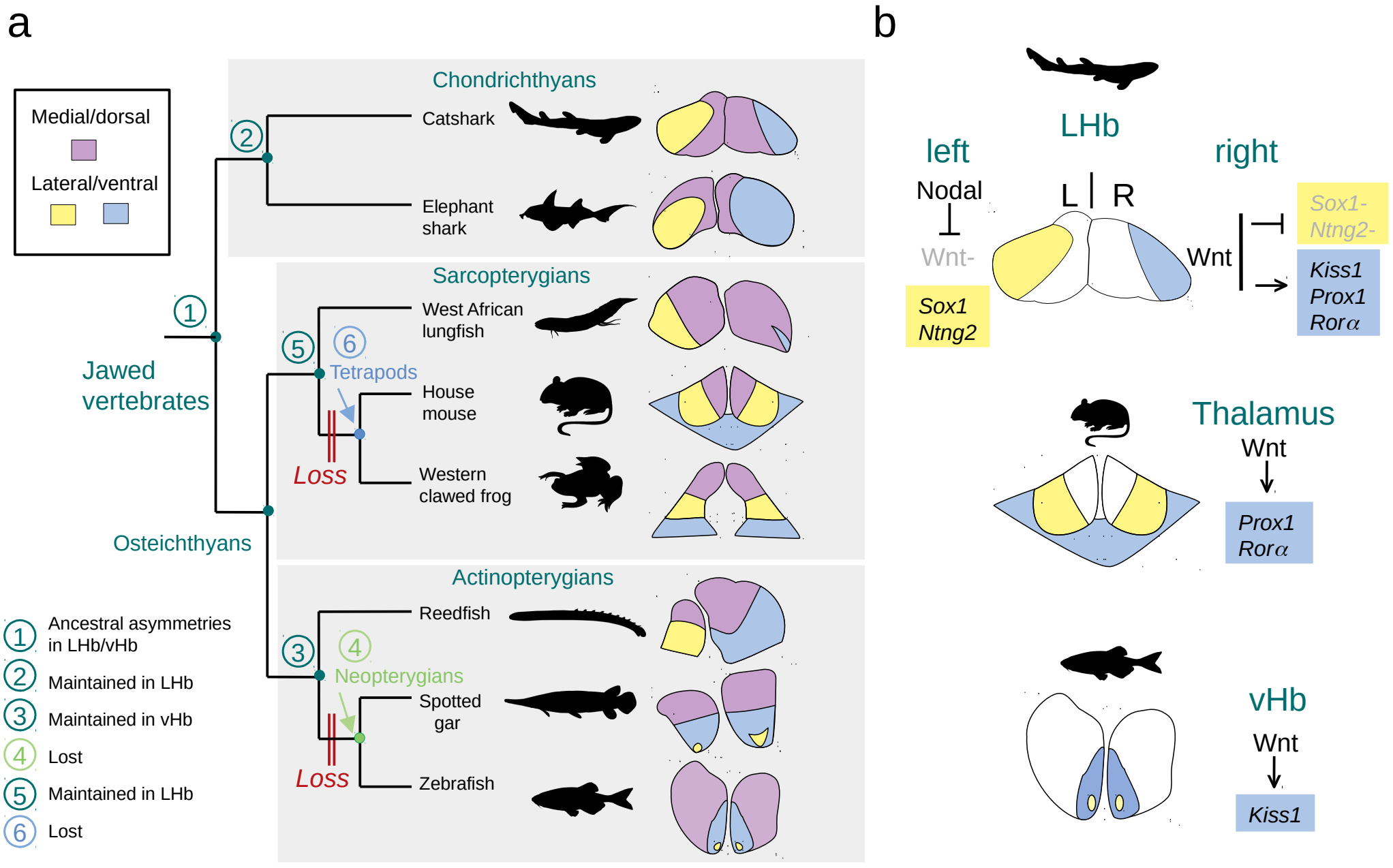
a
Medial/dorsal
Lateral/ventral
Chondrichthyans
Catshark
Elephant shark
Sarcopterygians
West African lungfish
Tetrapods
House mouse
Western clawed frog
Loss
Jawed vertebrates
Osteichthyans
Actinopterygians
Reedfish
Neopterygians
Spotted gar
Zebrafish
Loss
1 Ancestral asymmetries in LHb/vHb
2 Maintained in LHb
3 Maintained in vHb
4 Lost
5 Maintained in LHb
6 Lost
b
LHb
left
right
Nodal
Wnt-
Sox1
Ntng2
L
R
Wnt
Sox1-
Ntng2-
Kiss1
Prox1
Rorα
Thalamus
Wnt
Prox1
Rorα
vHb
Wnt
Kiss1

Figure 8